Angewandte Chemie
Eine Zeitschrift der Gesellschaft Deutscher Chemiker

Supporting Information

Dynamic Covalent Identification of an Efficient Heparin Ligand

*Miriam Corredor, Daniel Carbajo, Cecilia Domingo, Yolanda Pérez, Jordi Bujons, Angel Messeguer, and Ignacio Alfonso**

anie_201806770_sm_miscellaneous_information.pdf

Table of contents:

General methods

General: Reagents and solvents were purchased from commercial suppliers (Aldrich, Fluka or Merck) and were used without further purification. Flash chromatographic purifications and preparative reversed-phase purifications were performed on a Biotage® Isolera Prime™ equipment. TLCs were performed using 6x3 cm SiO_2 pre-coated aluminium plates (ALUGRAM® SIL G/UV_{254}).

Nuclear Magnetic Resonance (NMR): Spectroscopic experiments for the characterization of compounds were carried out on a Varian Mercury 400 instrument (400 MHz for ^{1}H and 101 MHz for ^{13}C). Chemical shifts (δ_H) are quoted in parts per million (ppm) and referenced to the appropriate NMR solvent peak(s). 2D-NMR experiments COSY, HSQC and HMBC were used where necessary in assigning NMR spectra. Spin-spin coupling constants (*J*) are reported in Hertz (Hz). For the experiments performed in aqueous buffer a low molecular weight heparin was used: **dp14** (from Iduron, prepared by high resolution gel filtration of partial heparin lyase digestion of high quality heparin, MW average ~ 4100). One- and two-dimensional (1D and 2D) NMR experiments were performed at 298 K on a 500 MHz Bruker AVANCEIII-HD equipped with a z-gradient (65.7 G cm^{-1}) inverse TCI-cryoprobe. Samples were dissolved in 5 mM Tris-d11 buffer with 50 mM NaCl (in D_2O, pH 7.5, uncorrected pH meter reading). Bruker TopSspin 3.5pl6 standard pulse sequences were used for 1D and 2D experiments. 2D ^{1}H-^{1}H experiments, TOCSY with zero-quantum suppression (DIPSI2GPPHZS, TM=70ms), NOESY with zero-quantum suppression (NOESYGPPHZS, TM=200ms) and TROESY (ROESYGPPH19.2, TM=250ms) were adquired for **3AL** with and without **dp14** heparin. Also, for **3AL** compound, 2D ^{1}H-^{13}C (HSQCETGPSISP2 and HMBCETGPL3ND) experiments were acquired. For full-length heparin-**3AL** titration (Figure S9), the CPMG spin-echo pulse sequence with pre-saturation (CPMGPR1D) was used, which follows the scheme: recycle delay – [–90°– (τ – 180° – τ)n – FID], with a τ = 'variable' and n = 'variable' (for a fixed CPMG loop cycle) as a T2-filter; these experiments were acquired with n fixed to 6 cycles and a τ value of 1ms.

Liquid Chromatography coupled to Mass Spectrometry: Analyses were carried out at the IQAC Mass Spectrometry Facility, using a UPLC-ESI-TOF equipment: [Acquity UPLC® BEH C_{18} 1.7 mm, 2.1x100 mm, LCT Premier Xe, Waters]. (CH_3CN + 20 mM HCOOH and H_2O + 20 mM HCOOH) mixtures at 0.3 mL/min were used as mobile phase.

Fluorescence spectroscopy: Fluorescence emission and excitation spectra were collected on a Photon Technology International Instrument, the Fluorescence Master Systems, using the Software Felix32 and cuvettes with 10 mm path length.

Dynamic covalent chemistry assays for the heparin ligand screening

A stock solution of imines was prepared by dissolving the necessary amounts of spermine and the aromatic aldehydes in MeOH rendering a final concentration of 10 mM in all the reagents. Then, two reaction mixtures were prepared in separate eppendorfs from the same stock solution of the imines by mixing 10 μL of the imine stock solution with 90 μL of a solution of 5mM $NaBH_3CN$ in aqueous 50 mM Tris Buffer at pH 7.5 (1mM final concentration of both spermine and each of the aldehydes) either in the absence or the presence of 1.2 mg of heparin (1 mM final concentration of heparin, ~17-18 mM on repeating unit). The mixtures were allowed to react at room temperature for 24 hours and after that quenched with 50 μL of 2M HCl, two-fold diluted with water and analyzed by UPLC-MS. The assignment of the peaks observed in the reactions was done on the basis of the m/z values and confirmed by injection of samples obtained from deconvoluted sublibraries. The amplification factors were calculated by dividing the normalized areas of the corresponding HPLC peaks in the presence of heparin (A_T) by the areas obtained in the absence of heparin (A_o). The results shown in Figure 1C of the manuscript are the average of three independent assays under the optimized reaction conditions.

The observed species were assigned by ion-detection UPLC-MS experiments.

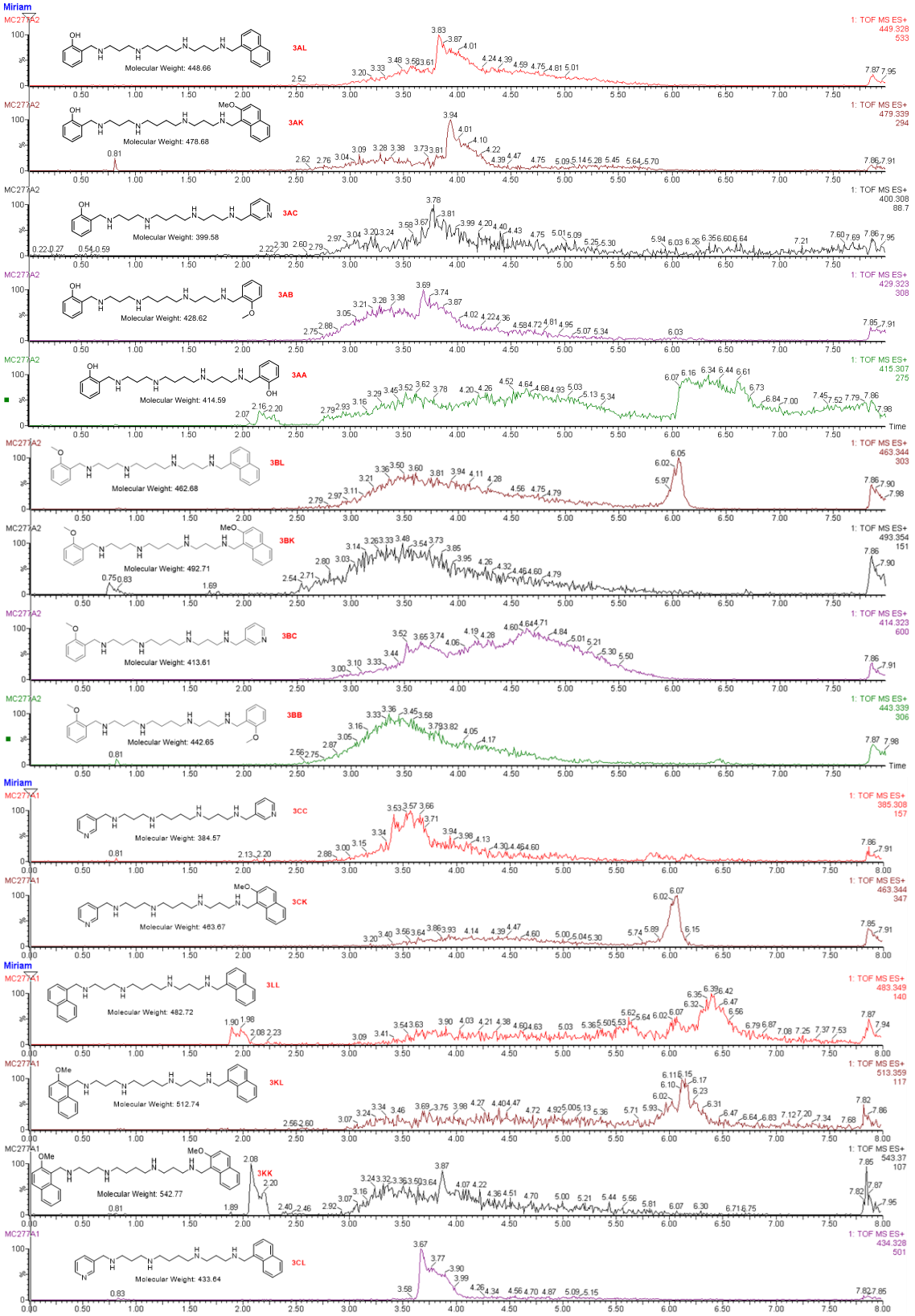

Figure S1. Ion-selective HPLC traces for each library member obtained from the reductive amination reaction in the absence of heparin. The two numbers on the right corner of each chromatogram correspond to the m/z values and the peak area, respectively.

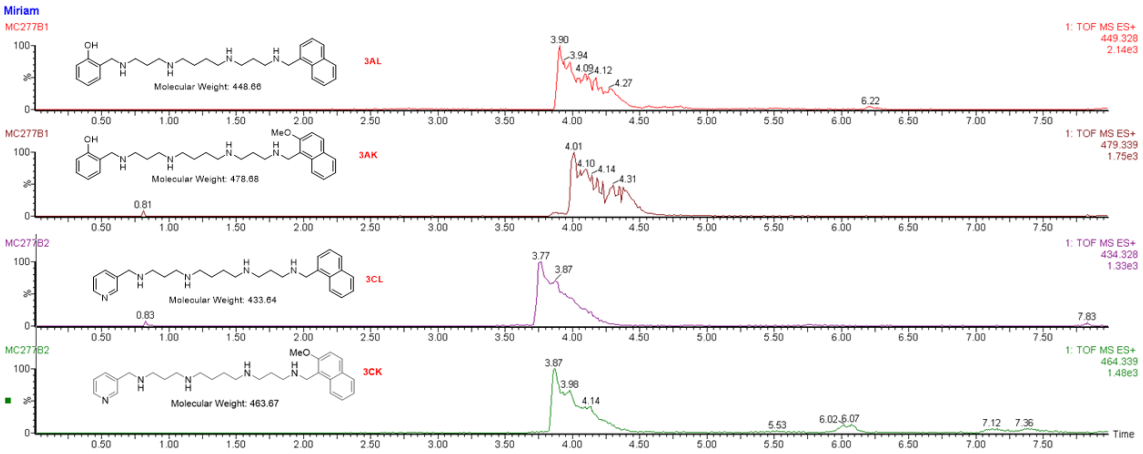

Figure S2. Ion-selective UPLC traces for selected library members obtained from the reductive amination reaction in the presence of heparin. The most amplified members are shown.

Preparative scale synthesis of the dialkylated spermine derivatives

Synthesis of symmetric compounds (**3AA** and **3LL**)

Synthesis of 3AA:

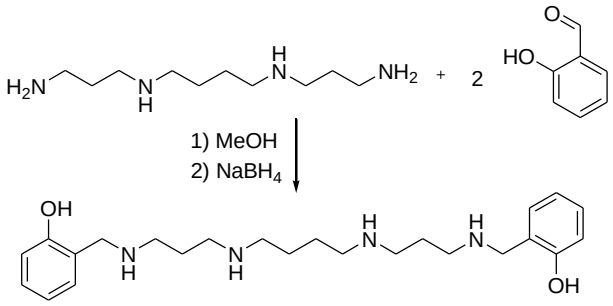

To a spermine (81 mg, 0.4 mmol) solution in MeOH (2 mL) a solution of salicylaldehyde (84 µL, 0.8 mmol) in MeOH (1 mL) was added drop by drop. The resulting reaction mixture was stirred overnight at ambient temperature. Then, $NaBH_4$ (120 mg, 8 eq) was added and the reaction was stirred for 6 hours. After addition of H_2O (1 mL) and HCl 2N (2 mL), the reaction mixture was stirred for 3 hours, evaporated and purified by reverse phase chromatography with a gradient of ACN (1% TFA) and water (1% TFA) to yield 134 mg (0.15 mmol, 38%) as a TFA salt with 95% purity.

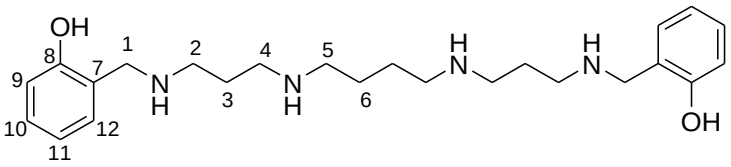

^{1}H-NMR (MeOD, 400 MHz): δ (ppm) 7.39-7.15 (m, 4H, H10,12), 7.03-6.78 (m, 4H, H9, 10), 4.22 (s, 4H, H1), 3.18-3.09 (m, 8H, H2,4), 3.07 (m, 4H, H5), 2.16 (m, 4H, 3H), 1.80 (m, 4H, H6) **^{13}C-NMR (MeOD, 100 MHz):** δ (ppm) 156.1 (C8), 131.1 (C10), 131.0 (C12), 119.6 (C11), 117.0 (C7), 114.9 (C9), 46.7 (C5), 46.6 (C1), 44.4 (C4), 43.8 (C2), 22.8 (C6), 22.5 (C3) **HRMS** for $C_{24}H_{39}N_4O_2$: Calculated: 415.3073 $(M+H)^+$; found: 415.3056.

HPLC and HRMS

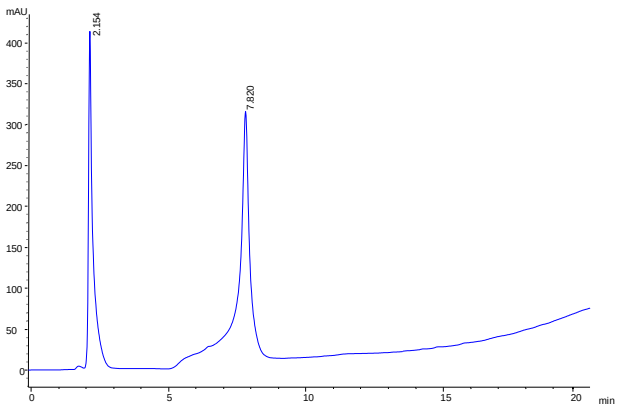

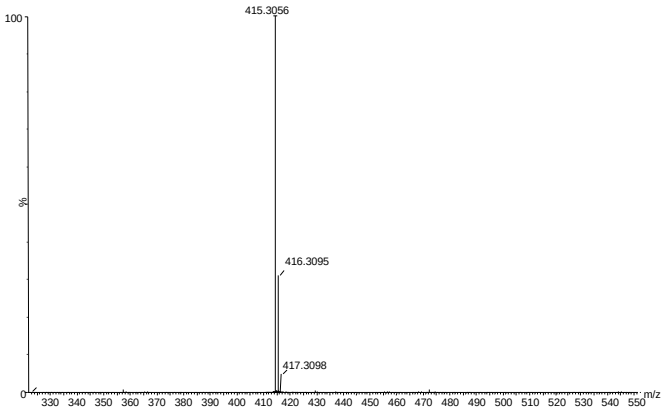

^{1}H NMR

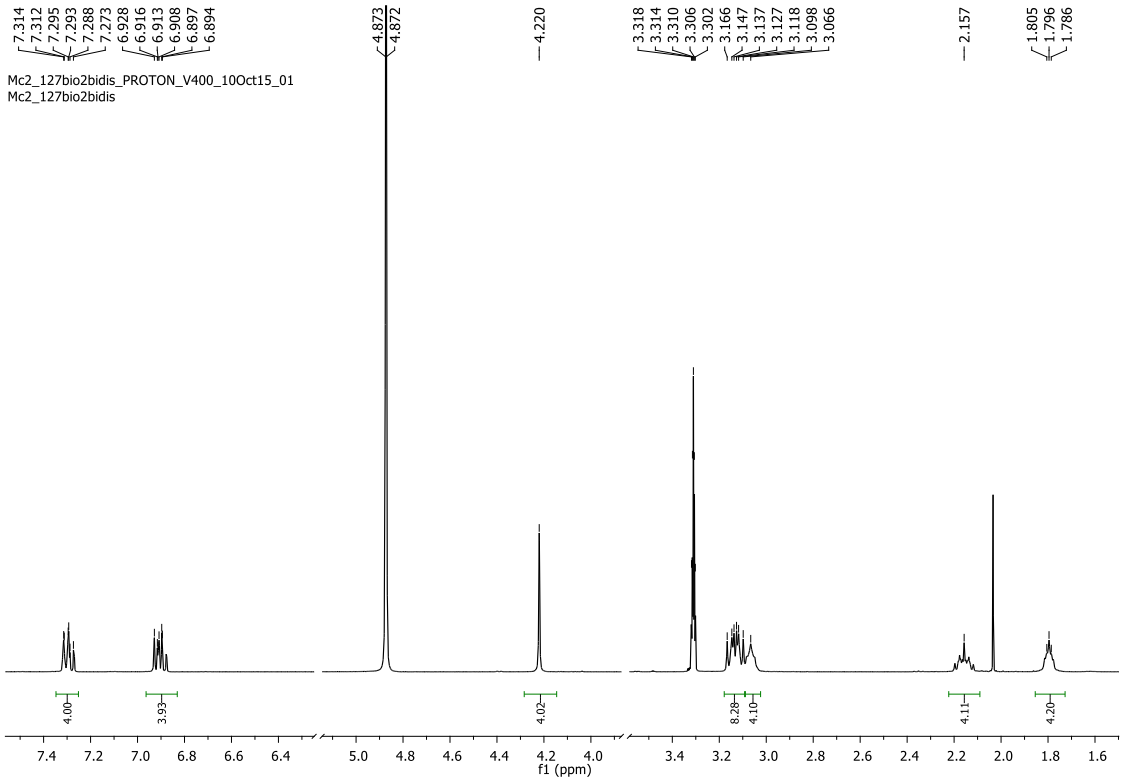

^{13}C NMR

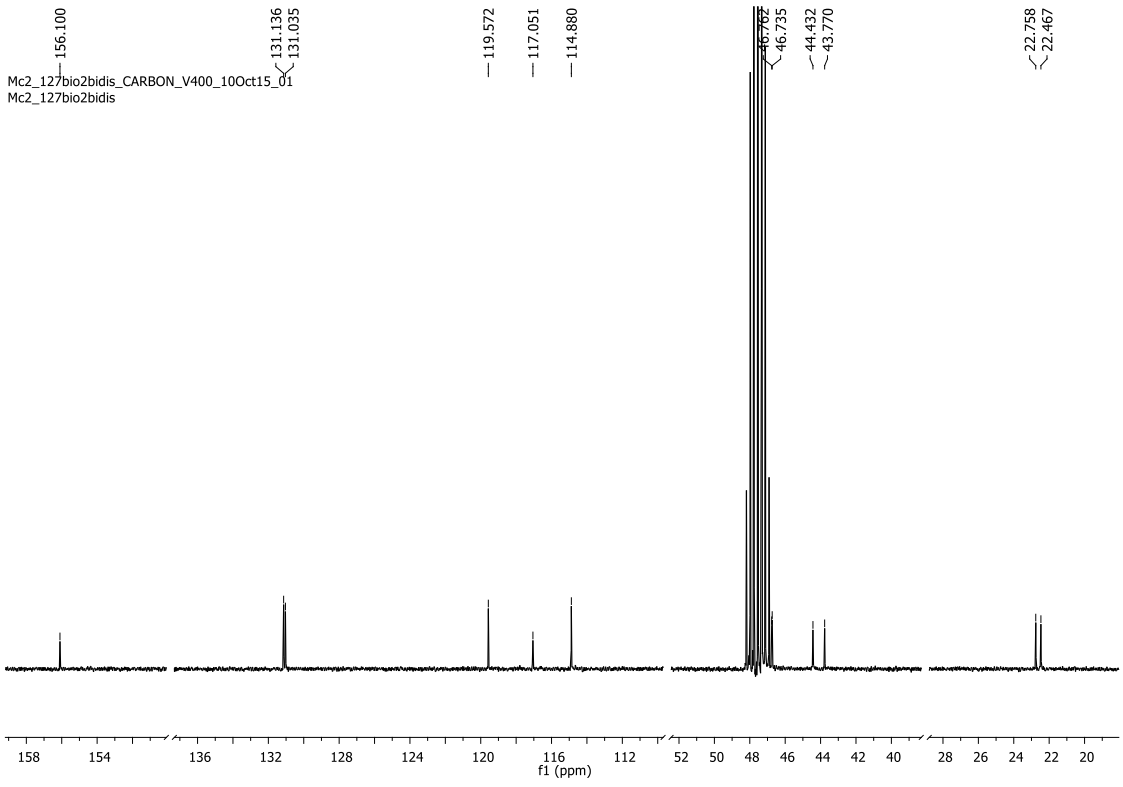

^{1}H-^{13}C HSQC

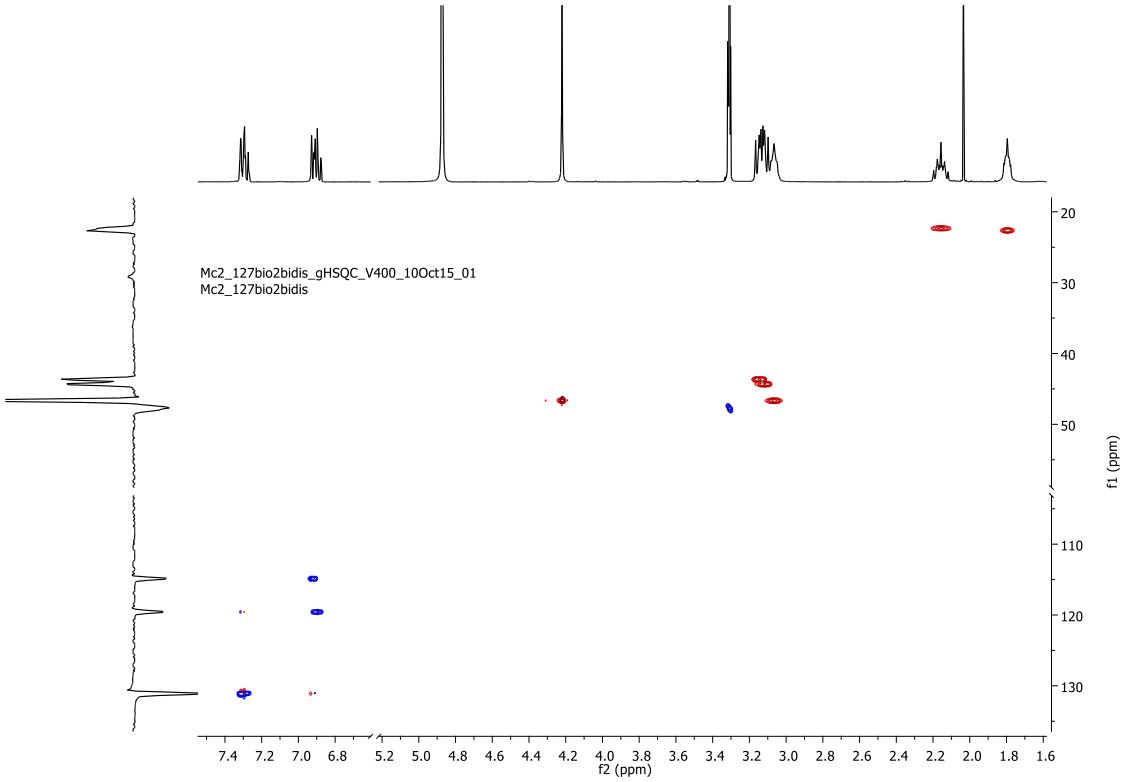

^{1}H-^{13}C HMBC

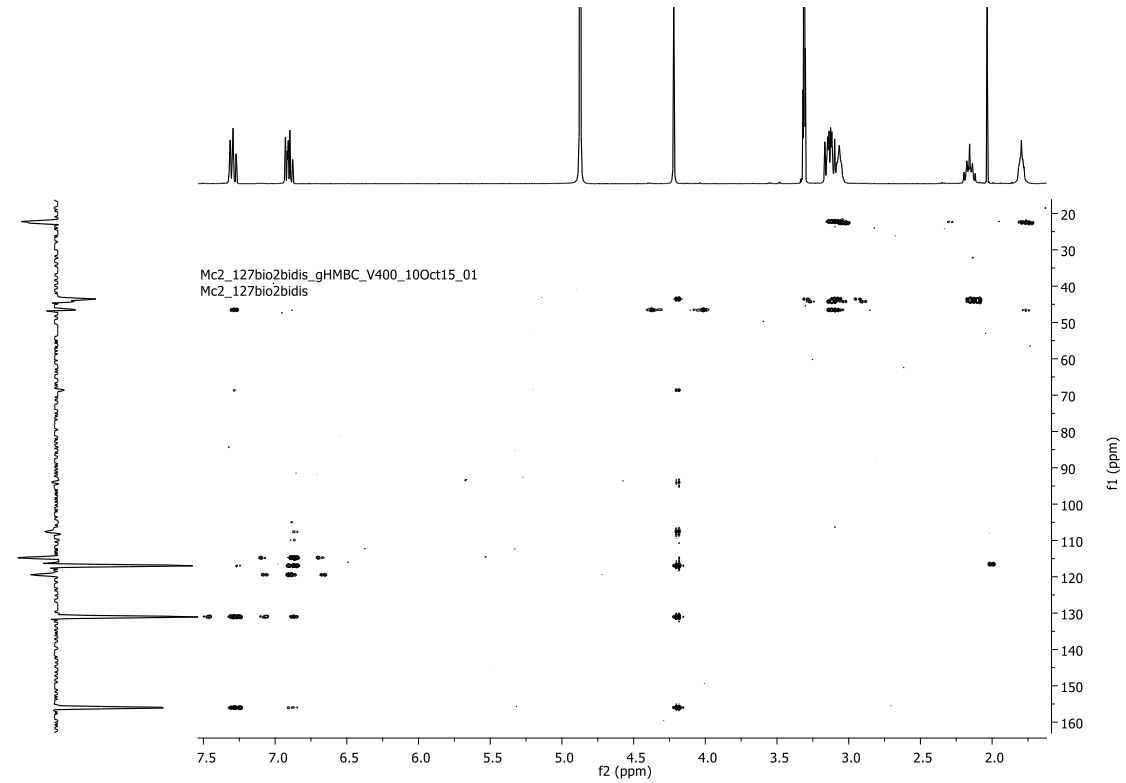

Synthesis of 3LL:

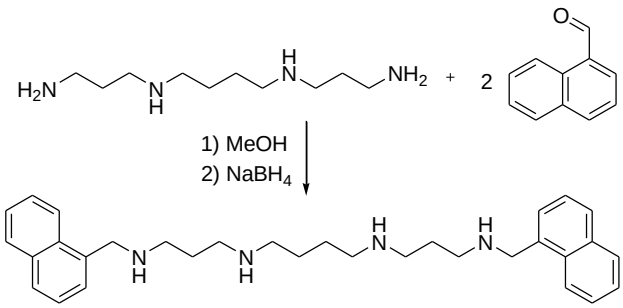

To a spermine (81 mg, 0.4 mmol) solution in MeOH (2 mL) a solution of 1-naphthylaldehyde (108 µL, 0.8 mmol) in MeOH (1 mL) was added. The resulting reaction mixture was stirred overnight at ambient temperature. Then, $NaBH_4$ (120 mg, 8 eq) was added and the reaction was stirred for 6 hours. After addition of H_2O (1 mL) and HCl 2N (2 mL), the reaction mixture was stirred for 3 hours, evaporated and purified by reverse phase chromatography with a gradient of ACN (1% TFA) and water (1% TFA) to yield 30 mg (0.03mmol, 8%) of product as a TFA salt with 95% purity, because the mono-substituted product is obtained during the reaction.

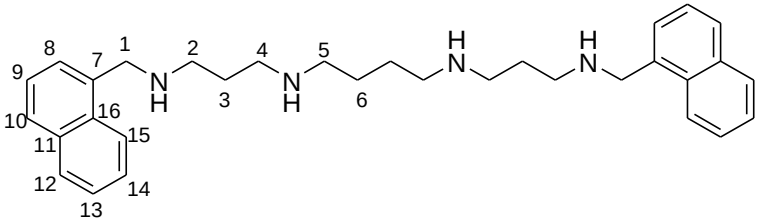

^{1}H-NMR (MeOD, 400 MHz): δ (ppm) 8.16 (d, *J* = 8.5 Hz, 2H, H15), 8.01 (dd, *J* = 10.0, 8.5 Hz, 4H, H10,12), 7.68 (ddd, *J* = 8.5, 7.0, 1.0 Hz, 4H, H8,14), 7.61 (ddd, *J* = 8.0, 7.0, 1.0 Hz, 2H, H13), 7.57 (dd, *J* = 8.0, 7.0 Hz, 2H, H9), 4.72 (s, 4H, H1), 3.29 (m, 4H, H2), 3.14 (m, 4H, H4), 3.07 (t, J = 6.8 Hz, 4H, H5), 2.18 (, 4H, H3), 1.79 (m, 4H, H6)
^{13}C-NMR (MeOD, 100 MHz): δ (ppm) 135.5 (C7), 132.6 (C11), 131.8 (C12), 130.4 (C8), 130.2 (C10), 128.5 (C14), 128.3 (C16), 127.7 (C13), 126.5 (C9), 123.7 (C15), 49.3 (C1), 48.1 (C5), 45.9 (C2), 45.8 (C4), 24.2 (C6), 24.1 (C3)
HRMS for $C_{32}H_{42}N_4$: Calculated: 483.3488 $(M+H)^+$; found: 483.3482

HPLC and HRMS

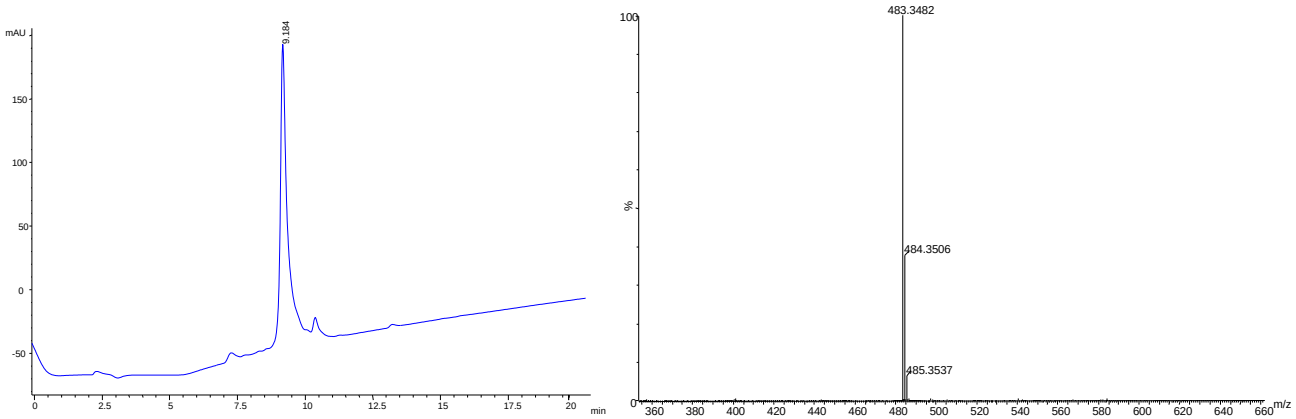

^{1}H NMR

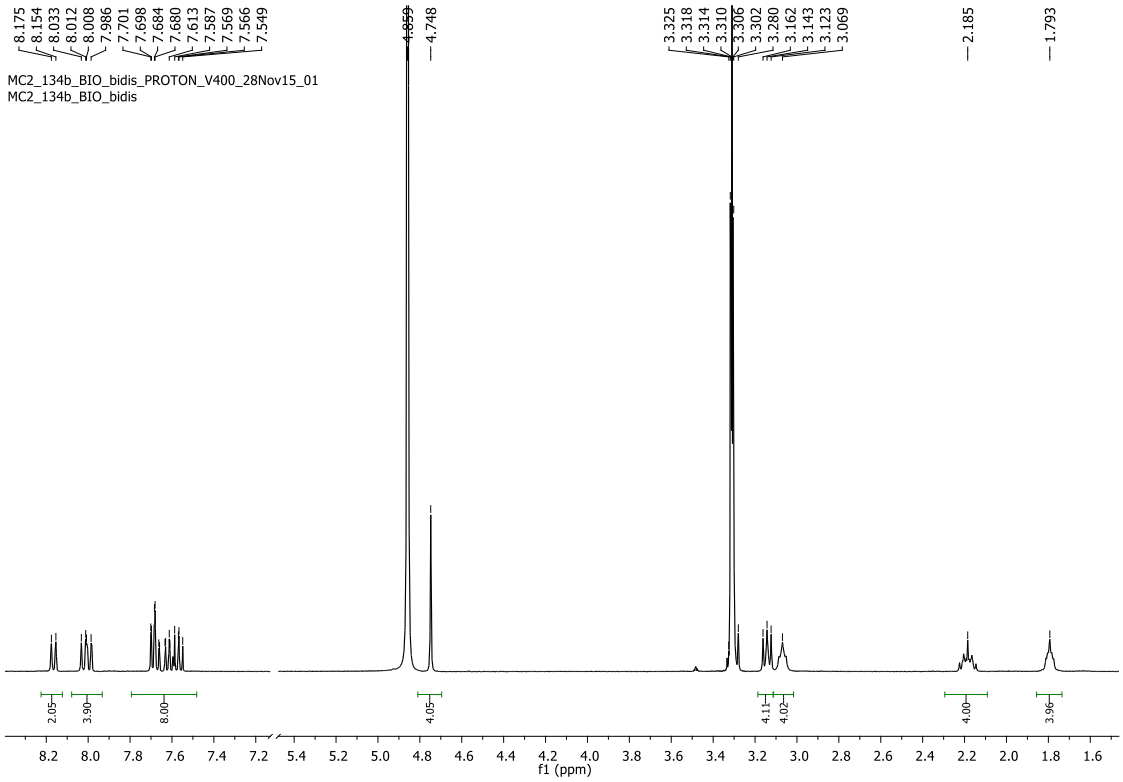

^{1}H-^{13}C HSQC

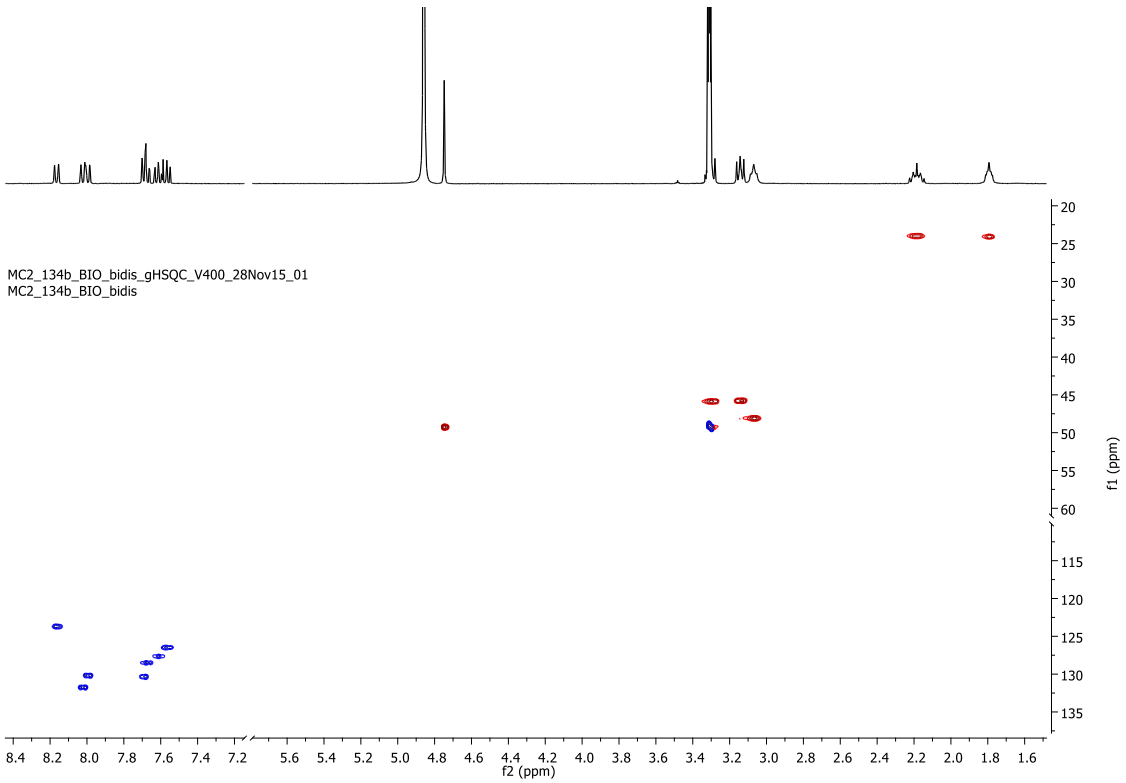

^{1}H-^{13}C HMBC

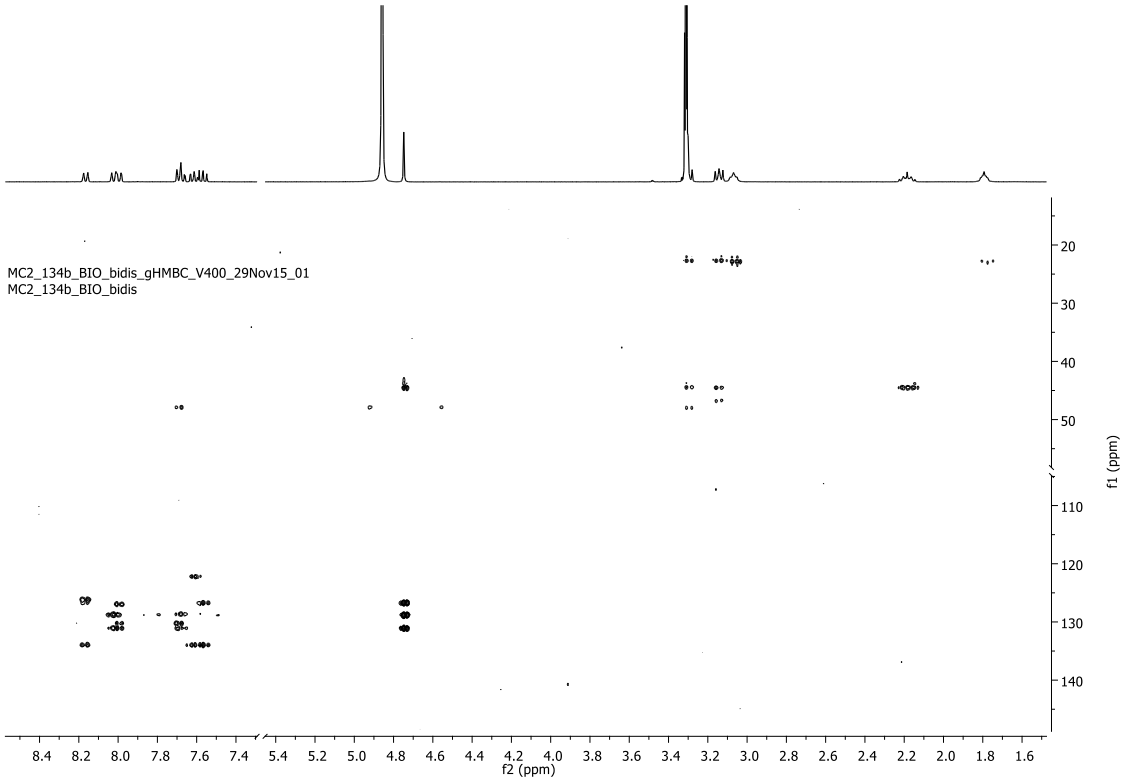
MC2_134b_BIO_bidis_gHMBC_V400_29Nov15_01
MC2_134b_BIO_bidis
f2 (ppm)
f1 (ppm)

Synthesis of asymmetric compound 3AL

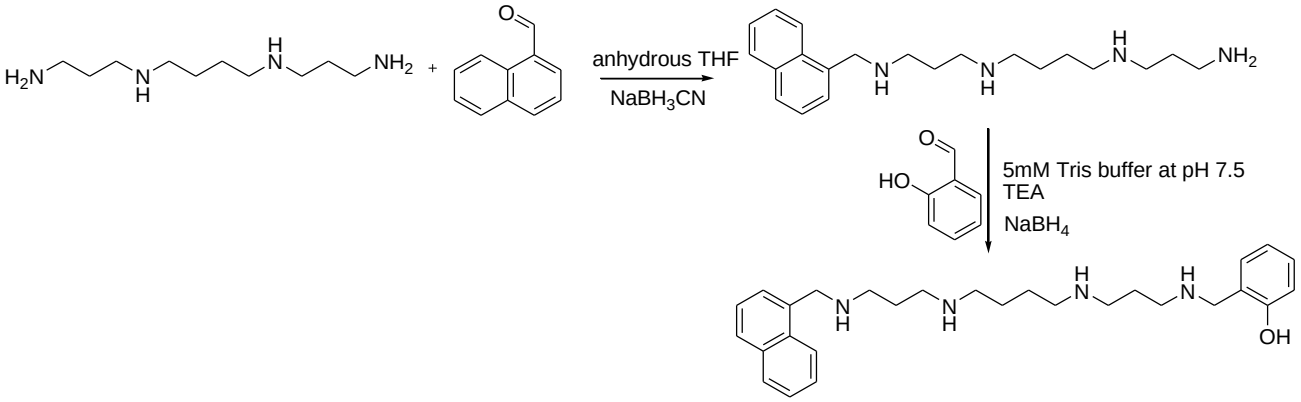

Monoalkylated spermine with aldehyde L (3L): To an ice-solution of spermine (121 mg, 0.6 mmol) in anhydrous THF (2 mL), a solution of 1-naphthylaldehyde (54 µL, 0.4 mmol) was added dropwise. The resulting reaction mixture was stirred at ambient temperature overnight. Then $NaBH_3CN$ (201 mg, 3.2 mmol) was added and the reaction was stirred overnight. After the addition of 1 mL of H_2O, the reaction was stirred one hour, and then 2mL of HCl (2N) were added and the reaction mixture was stirred for two more hours. The crude was purified by reverse phase chromatography leading 44 mg (0.07 mmol, 18% yield) of final product as a TFA salt.

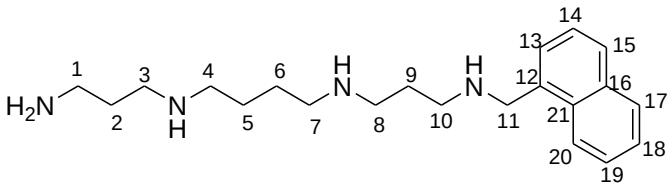

^{1}H-NMR (MeOD, 400 MHz): δ (ppm) 8.17 (d, *J* = 8.5 Hz, 1H, H20), 8.10-7.94 (m, 2H, H15,17), 7.80-7.64 (m, 2H, H13,19), 7.64-7.50 (m, 2H, H14,18), 4.72 (s, 2H, H11), 3.3 (m, 2H, H10), 3.20-3.10 (m, 4H, H3,8), 3.10-3.0 (m, 6H, H1,4,7), 2.19 (m, 2H, H9), 2.09 (m, 2H, H2), 1.80 (m, 4H, H5,6 **^{13}C-NMR (MeOD, 100 MHz):** δ (ppm) 135.5 (C12), 132.7 (C16), 131.7 (C17), 130.4 (C21), 130.3 (C19), 130.2 (C15), 128.5 (C13), 127.7 (C18), 126.5 (C14), 123.8 (C20), 49.3 (C11), 48.2 (C4,7), 46.1 (C10), 45.9 (C3,8), 37.8 (C1), 25.4 (C2), 24.2 (C5,6), 24.1 (C9) **HRMS** for $C_{21}H_{34}N_4$: Calculated: 343.2862 $(M+H)^+$; found: 343.2820.

HPLC and HRMS

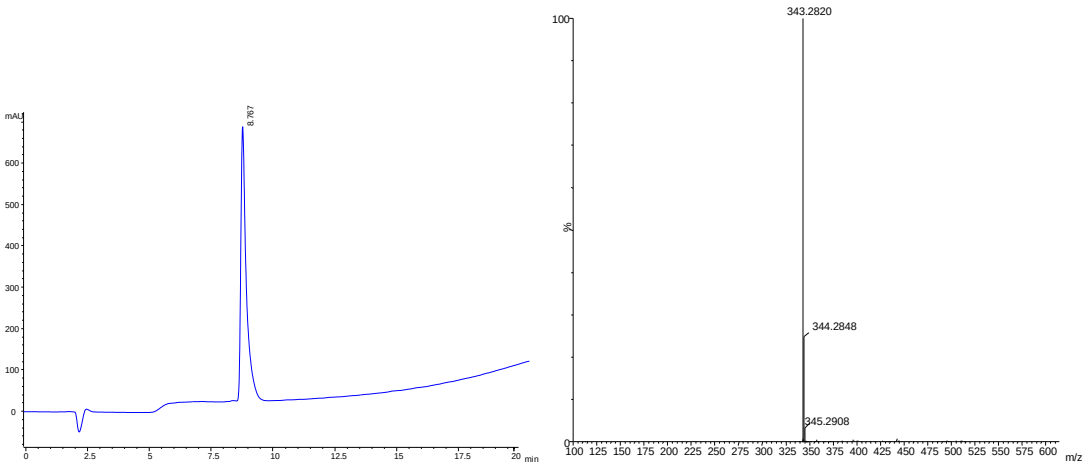

^{1}H NMR

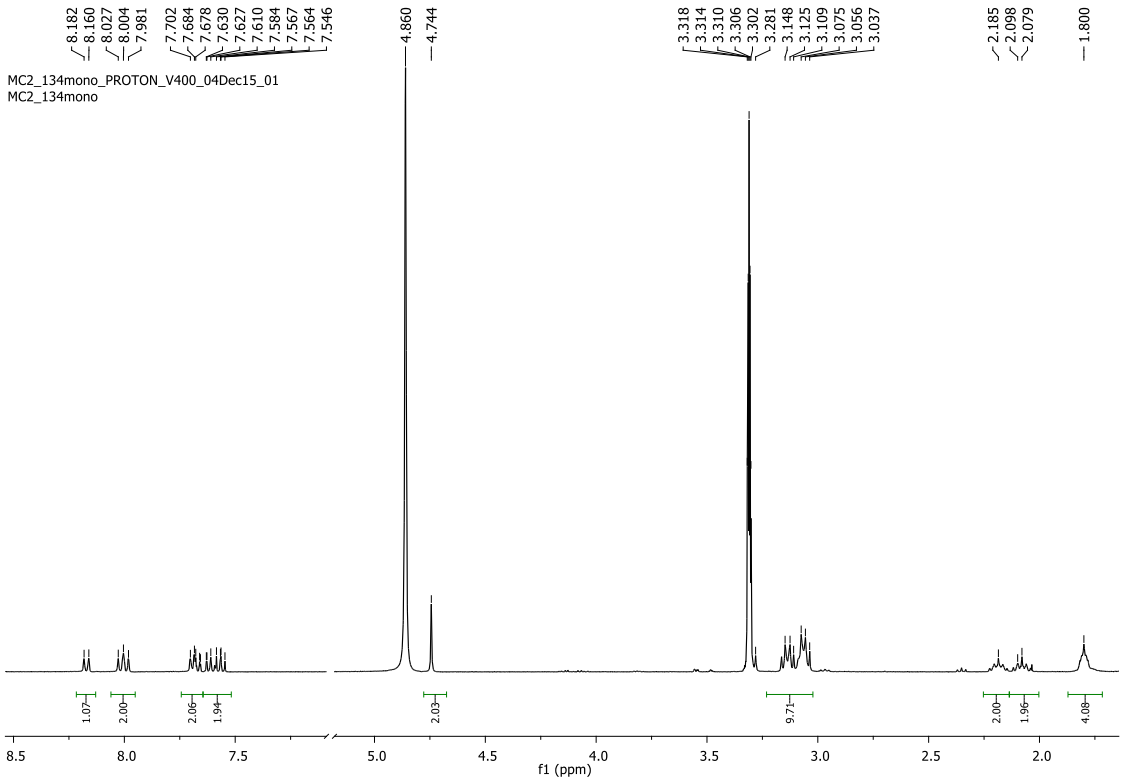

^{13}C NMR

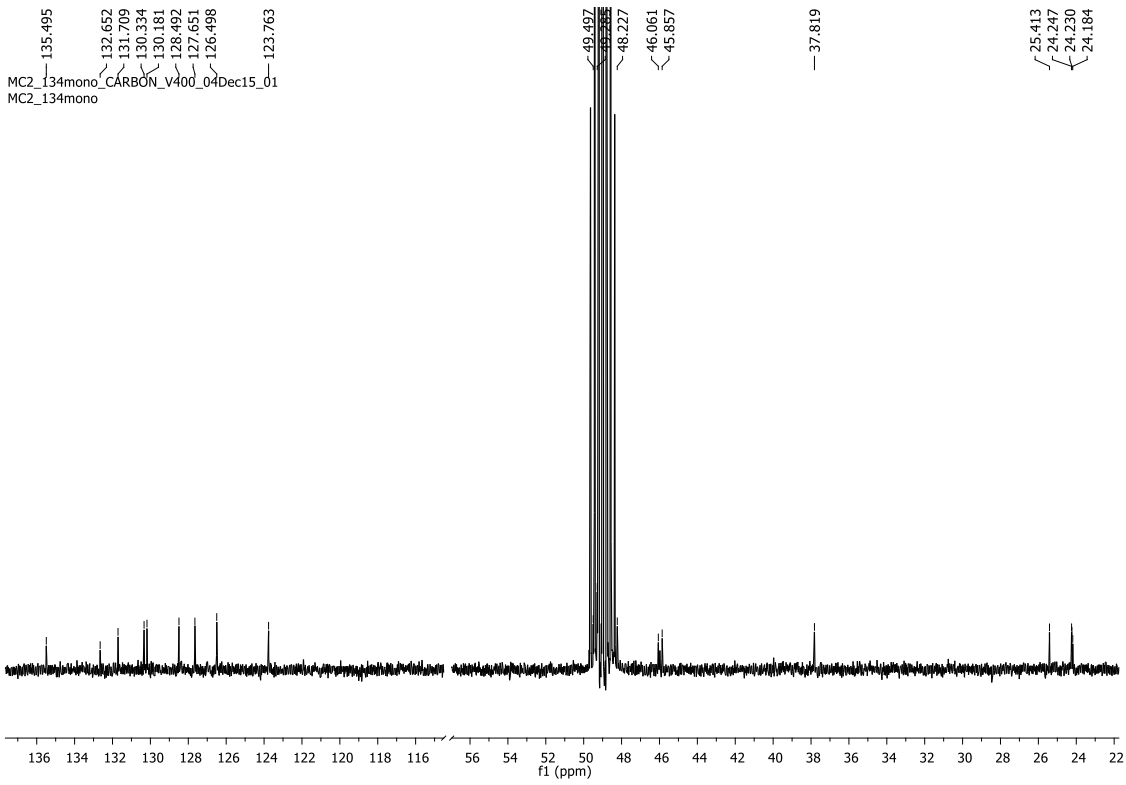

^{1}H-^{1}H gCOSY

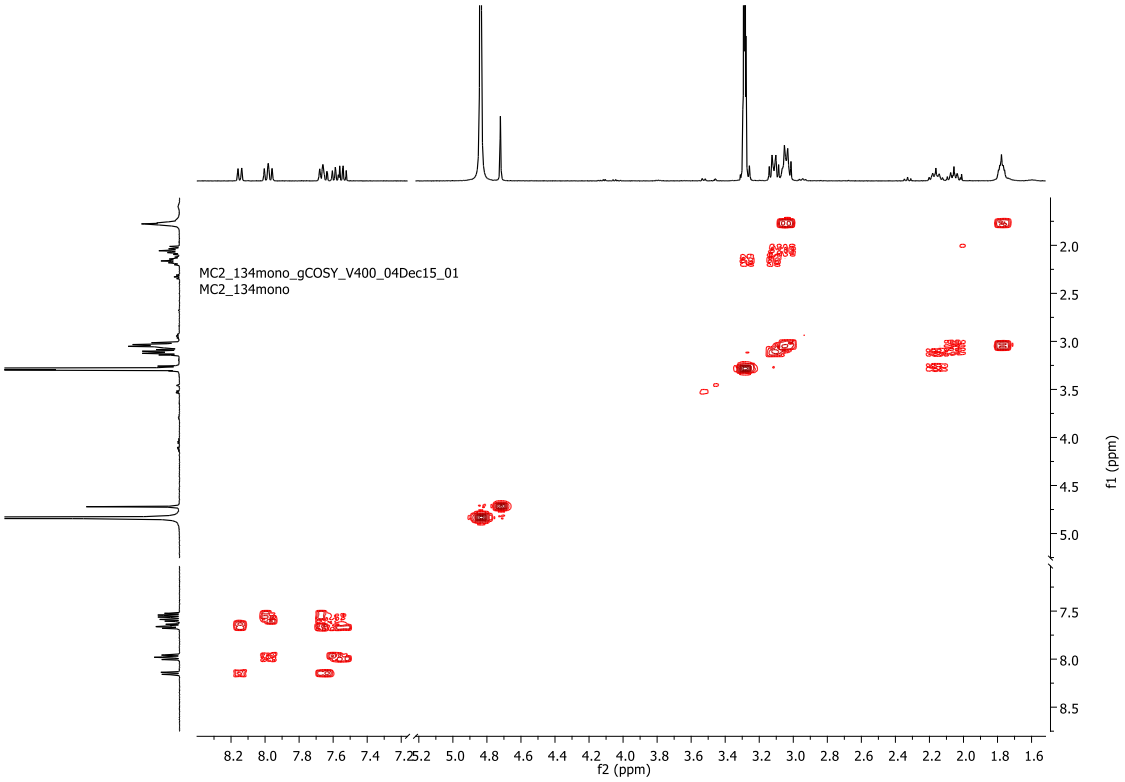

^{1}H-^{13}C gHSQC

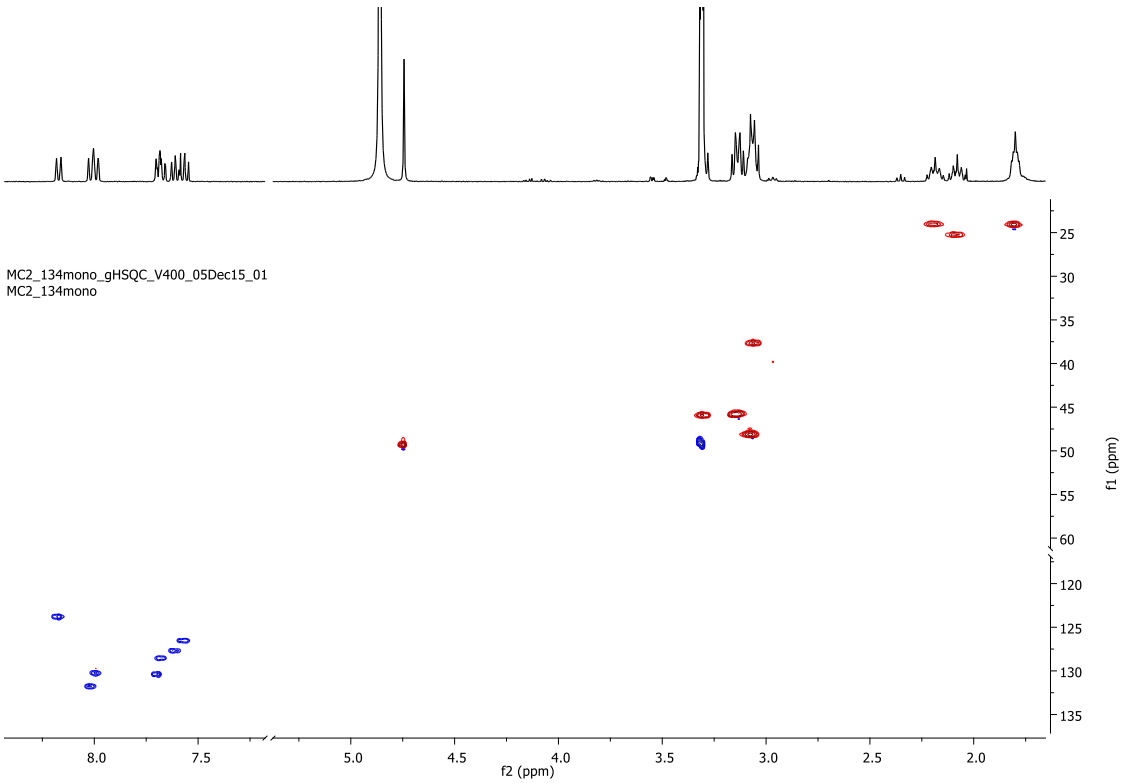

^{1}H-^{13}C gHMBC

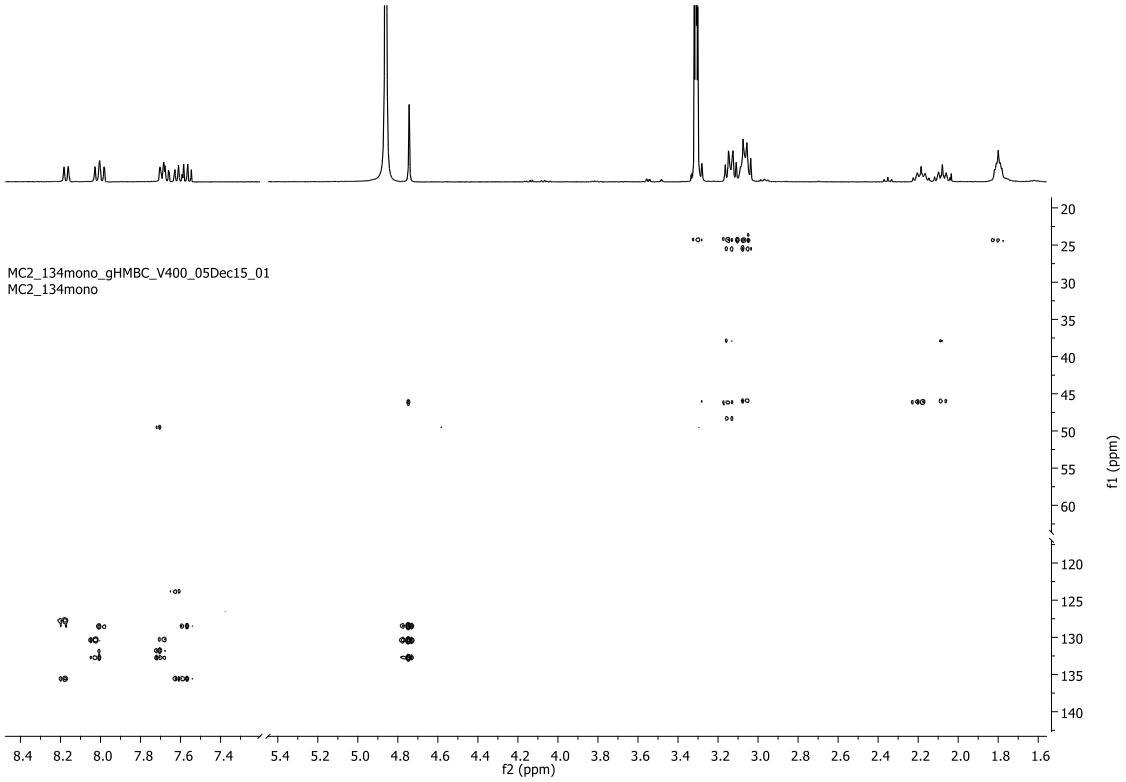

Synthesis of 3AL: To a solution of the amine **3L** (44mg, 0.07 mmol) in 1 mL of Tris buffer at pH 7.5, TEA (20 µL, 2eq) and salicylaldehyde (6.5 µL, 0.06 mmol) were added. The mixture was stirred overnight at room temperature. Then $NaBH_4$ (10 mg, 4 eq) was added and the reaction mixture was stirred for 6 hours.

The reaction was treated with HCl 2N (2 mL) and stirred for two hours, after evaporating the solvent, it was purified by reverse phase chromatography using a gradient of ACN (1%TFA) and water (1% TFA) to yield 10 mg (0.01 mmol, 18%) of the final product as a TFA salt.

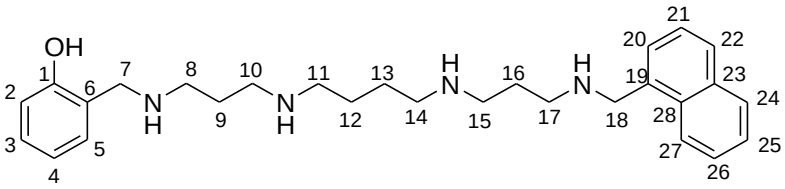

^{1}H-NMR (MeOD, 400 MHz): δ (ppm) 8.17 (d, J = 8.0 Hz, 1H, H27), 8.01 (dd, J = 10.0, 8.5 Hz, 2H, H22,24), 7.79-7.65 (m, 2H, H20,26), 7.64-7.49 (m, 2H, H21,25), 7.29 (m, 2H, H3,5), 6.91 (m, 2H, H2,4), 4.75 (s, 2H, H18), 4.22 (s, 2H, H7), 3.31 (m, 2H, H17), 3.14 (m, 6H, H8,10,15), 3.08 (m, 4H, H11,14), 2.17 (m, 4H, H9,16), 1.79 (m, 4H, H12,13) **^{13}C-NMR (MeOD, 100 MHz):** δ (ppm) 157.5 (C1), 135.5 (C19), 132.7 (C23), 132.6 (C3), 132.5 (C5), 131.8 (C24), 130.4 (C20), 130.2 (C22), 128.5 (C26), 128.2 (C28), 127.7 (C25), 126.5 (C21), 123.7 (C27), 121.1 (C4), 118.5 (C6), 116.4 (C2), 49.2 (C18), 48.2 (C7), 48.2 (C11,14), 45.9 (C17), 45.8,45.2 (C8,10,15), 24.2 (C12,13), 24.1 (C16), 23.9 (C9) **HRMS** for $C_{28}H_{40}N_4O$: Calculated: 449.328 $(M+H)^+$; found: 449.3281.

HPLC and HRMS

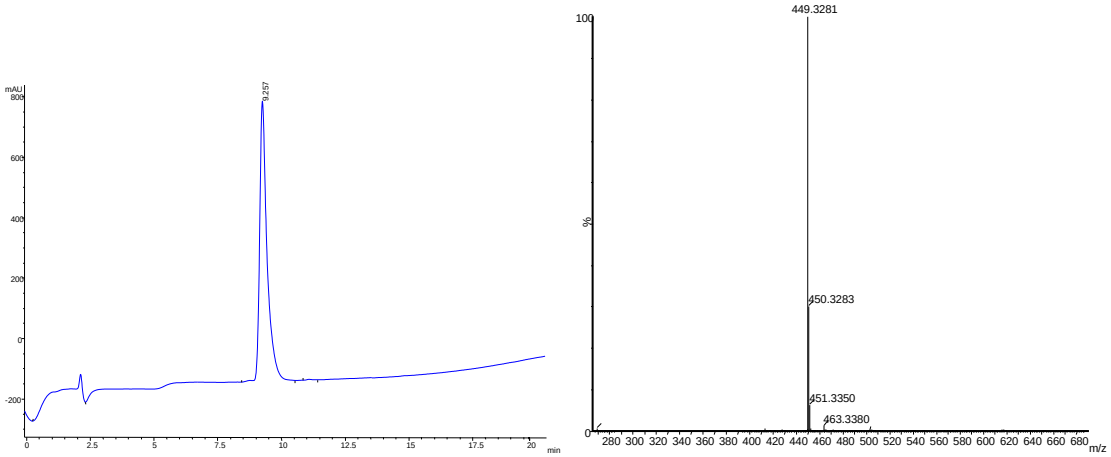

^{1}H NMR

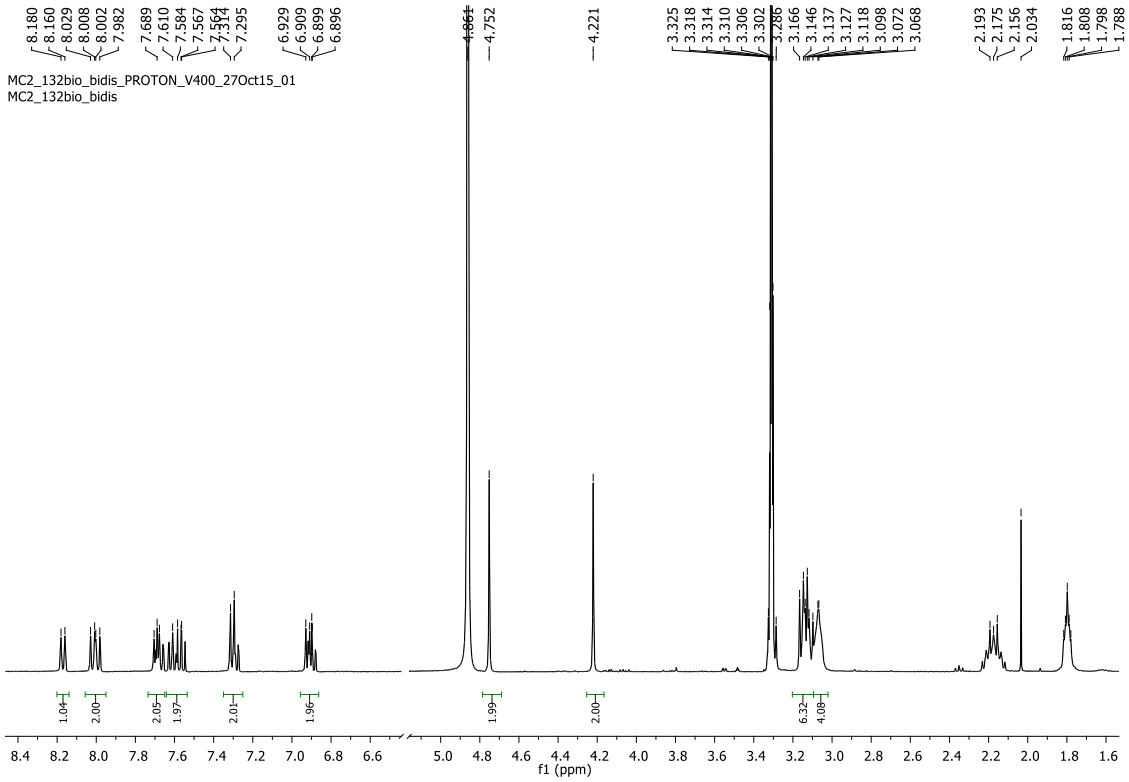

^{13}C NMR

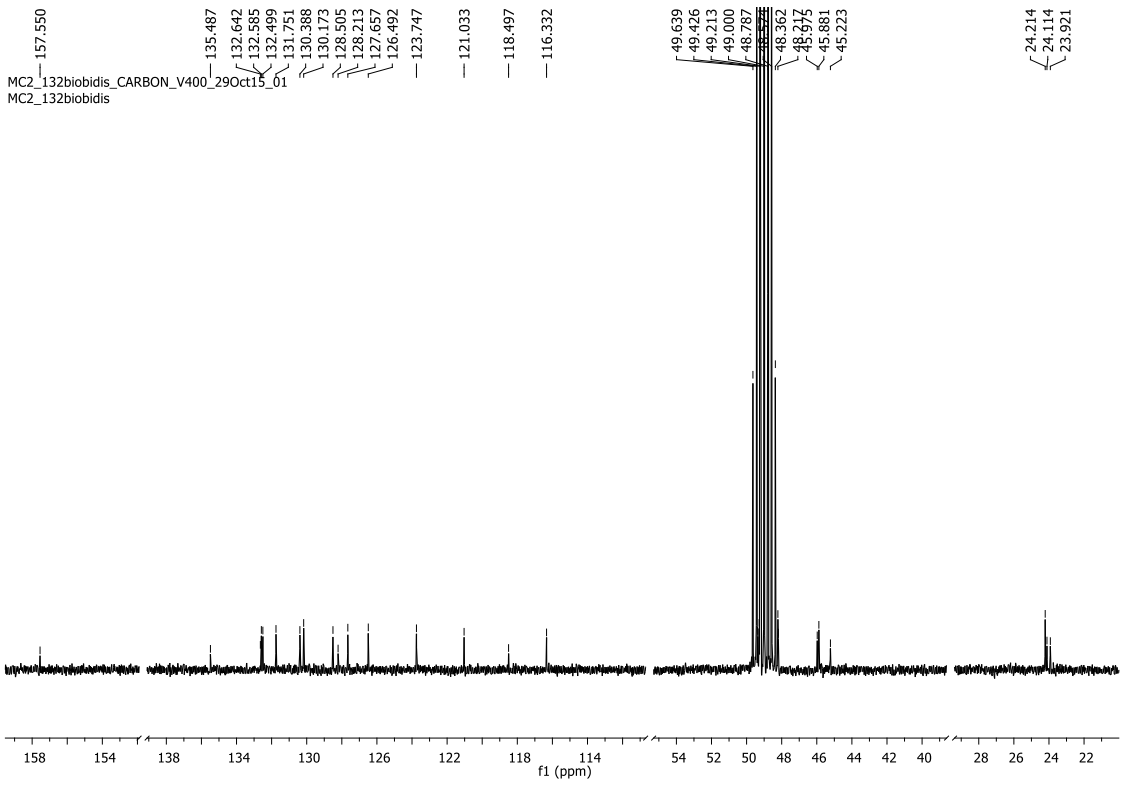

^{1}H ^{13}C HSQC

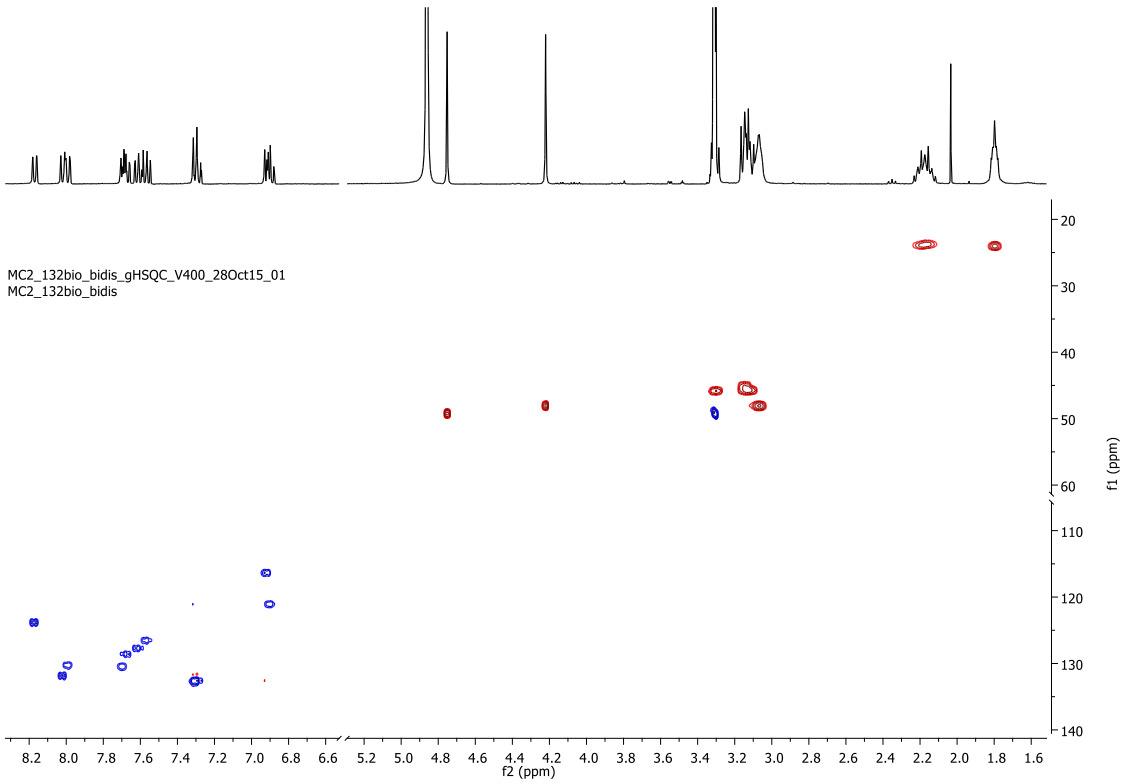

^{1}H ^{13}C HMBC

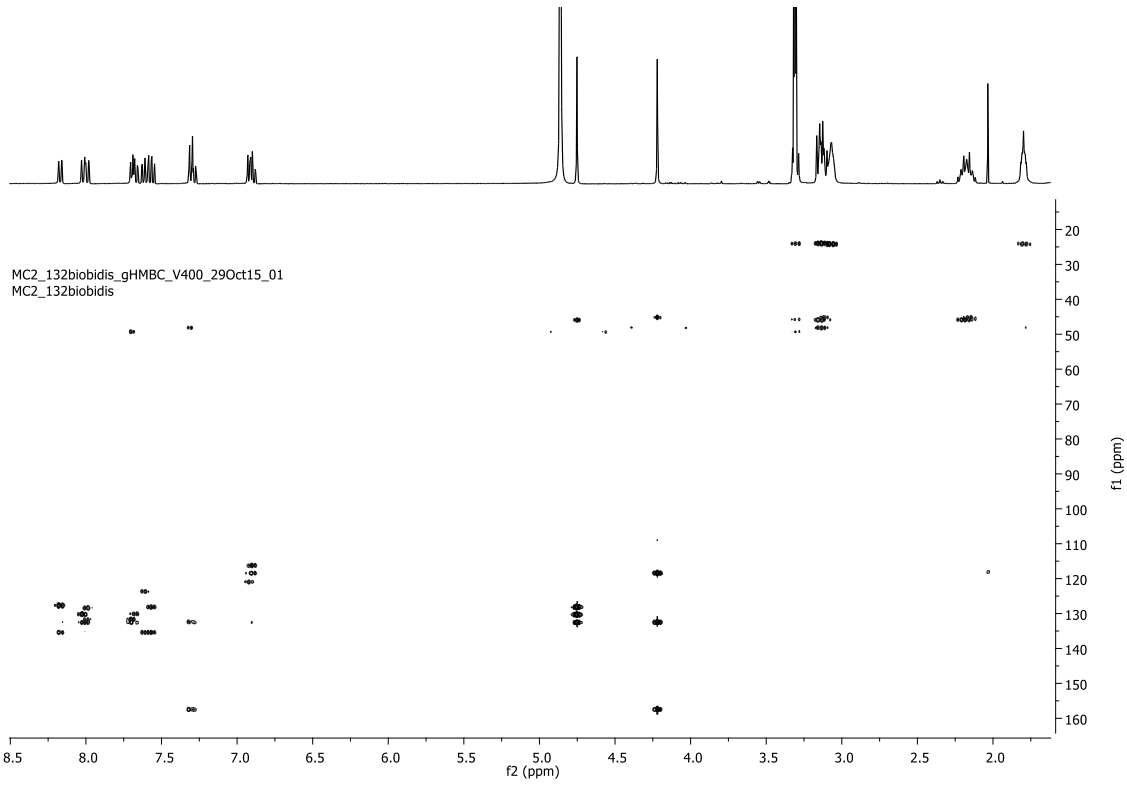

Fluorescence titration experiments

Stock solutions of the corresponding ligand (49 μM) and heparin (0.4 mM in the disaccharide repeating unit) were prepared in 5 mM Tris buffer at pH 7.5. 2 mL of the ligand solution was placed on a quartz cell and the emission fluorescence spectrum was measured upon excitation at 280 nm. Then, small volumes of the heparin stock solution were added to the cell, and the fluorescence spectra was acquired after each addition. The normalized relative fluorescence increase of the intensity at 400 nm was plotted against the equivalents of heparin added, considering the concentration of the repeating disaccharide unit. The titration isotherm showed a complex shape that was impossible to reliably fit to a reasonable binding model. However, the qualitative comparison between the **3AL** and **3LL** curves showed a stronger interaction of heparin with **3AL**. Thus, the titration of **3AL** reaches the maximum fluorescence change at 2.5 equivalents of repeating units of **1**, while the curve for **3LL** is still growing at 4 equivalents of repeating units of **1**. Moreover, the steepness of the titration isotherm of **3AL** is much larger than that of **3LL**, suggesting a higher degree of complex formation with equivalent proportion of added heparin.

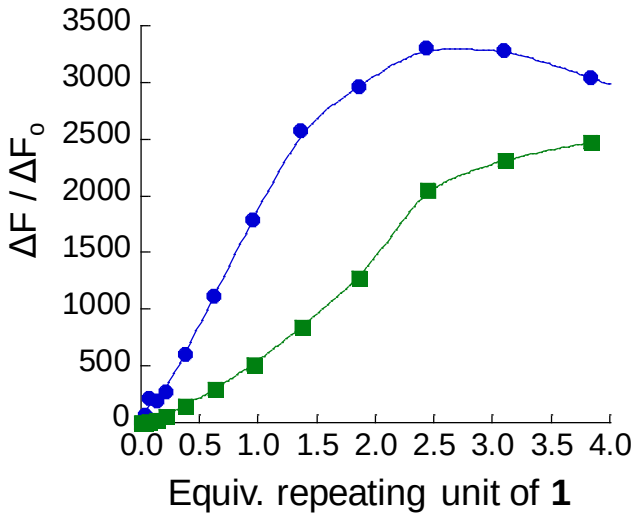

Figure S3. Fluorescence titration curves for **3AL** (blue) and **3LL** (green) upon addition of **1**

Isothermal Titration Calorimetry experiments

ITC was performed in a MicroCal VP-ITC instrument (GE Healthcare) in 5 mM Tris-HCl buffer pH 7.5 at 298 K. The cell (volume ~ 1.4 mL) contained 80 µM of the ligand while the syringe (volume ~ 0.3 mL) contained 200 µM heparin (considering the average molecular weight of the corresponding polysaccharide). Experimental conditions were as follows: a first injection of 2 µL followed by 40 injections of 5 µL with a spacing of 180 s between injections, and a stirring speed of 300 rpm. A blank titration was performed by injecting buffer into the products in the same conditions. Raw data were analyzed with the MicroCal Origin software (OriginLab, Northampton, MA, USA) using a one-site model for the fittings.

For the calculation of the molar concentration of heparin, we considered the averaged MW of the specific heparin used (12 kD), despite it was polydisperse. The influence of the heparin heterogeneity on the determined parameters was not limiting in our case, since our objective was to estimate the affinity and to compare the results for the different ligands under the same conditions.

ITC experiments with 3AL

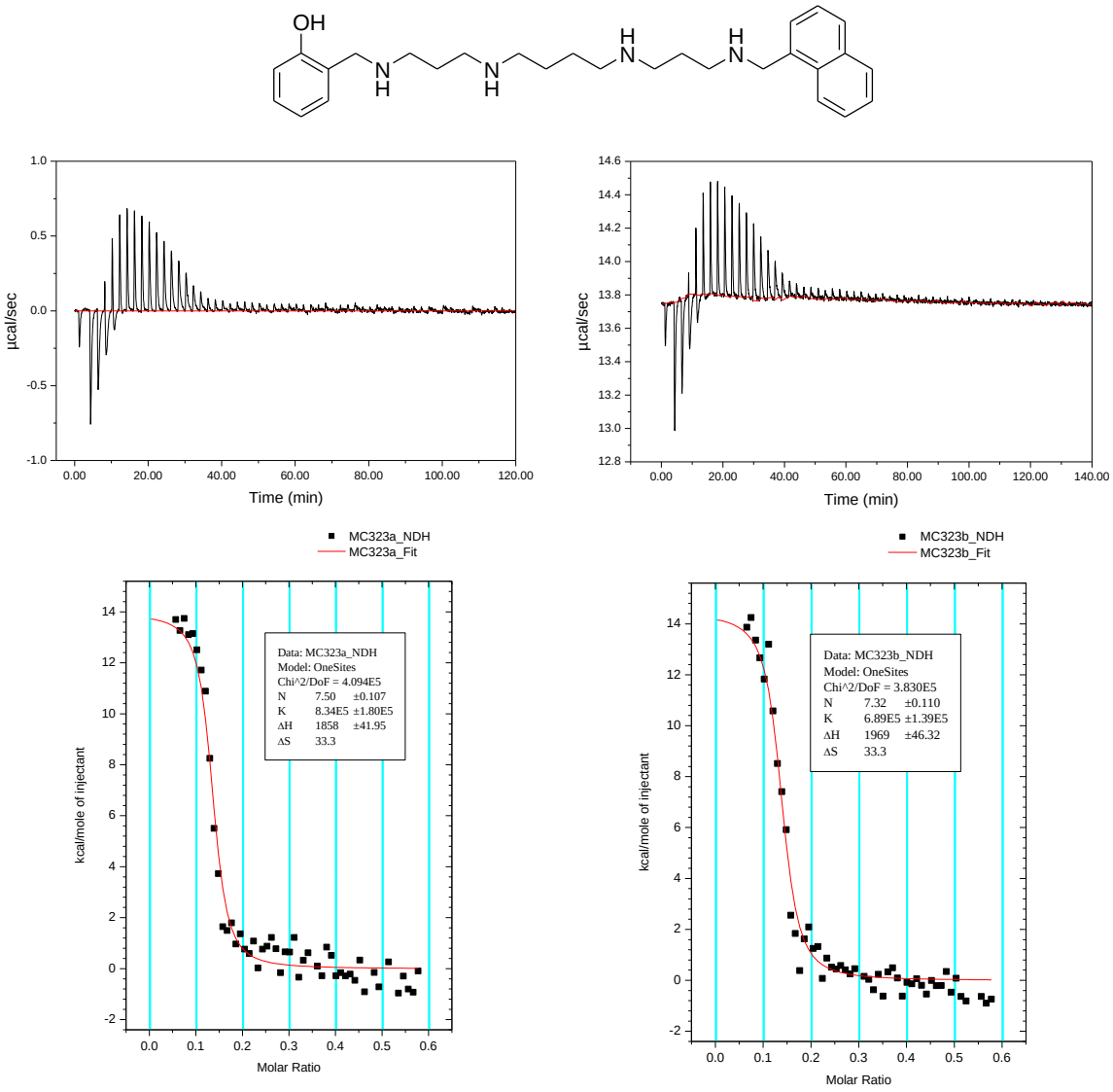

Figure S4. Raw data (up) and processed data (down) for two ITC experiments of **3AL** with heparin.

The ITC curves showed an exothermic process in the initial titration points and a consistent endothermic process after a certain point of the titration. This behavior has been previously observed in the titration of

GAGs with cationic peptides[1] and peptidomometics,[2] and can be ascribed to an initial non-specific aggregation process by purely electrostatic interactions. In this case, we have confirmed this aggregation with two additional independent experiments. First, the ^{1}H NMR titration of **3AL** with non-fractioned heparin, using a relaxation-filtering pulse sequence (Figure S12) showed the disappearance of the NMR signals of **3AL** in the first titration points, which is consistent with the formation of very large species in solution with a very fast cross-relaxation (short T_2 and thus efficiently filtered with the CPMG sequence). The signals of the **3AL** ligand were recovered upon further addition of heparin, suggesting the formation of discrete species with smaller apparent sizes. These discrete species would correspond to the ligand-to-heparin ratios of the consistent endothermic process observed in the ITC curves.

In order to confirm this hypothesis, we have measured the dynamic light scattering (DLS) of samples containing **3AL** and **1** at relative concentrations similar to those of the first points of the ITC titrations (20 µM of **3AL** and 0.2 µM of heparin, corresponding to 3.4-3.6 µM in the disaccharide repeating unit). The DLS data confirmed the formation of very large species of a hydrodynamic radius of 61 ± 4 nm and a polydispersity of 0.3 ± 0.2. The DLS of the corresponding samples of either **3AL** or heparin alone showed no scattering in separate control experiments. Thus, we concluded that the first points of the titration experiments correspond to large aggregates formed by non-specific electrostatic interactions between **3AL** and **1** and, accordingly, we used just the endothermic points for the fitting. Despite this is an oversimplification of the true process, we considered that the obtained data can be used for comparison purposes.

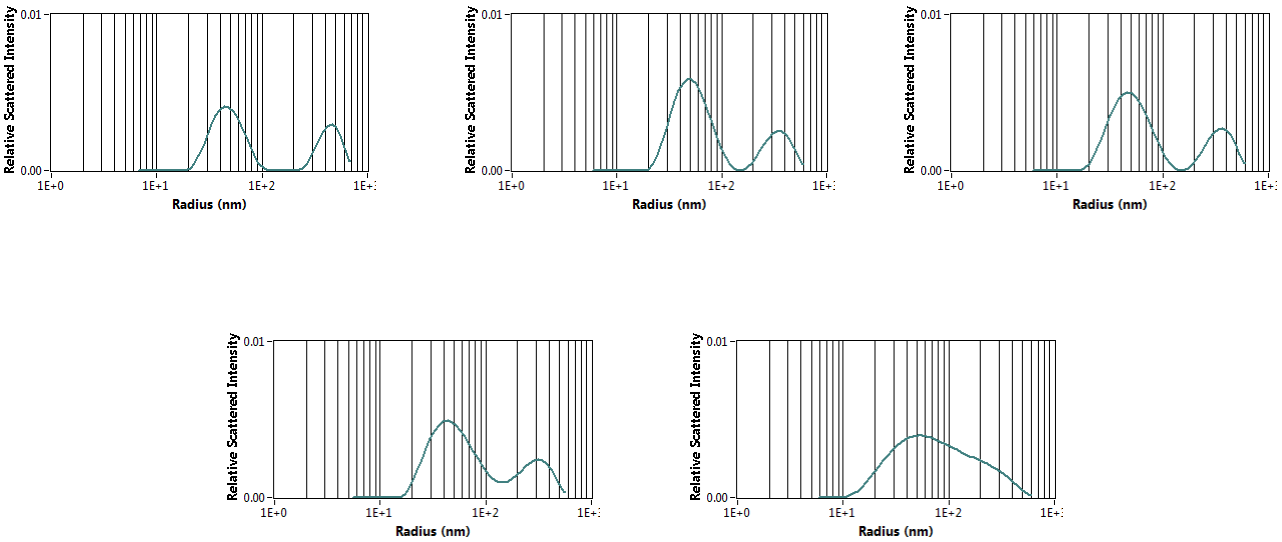

Figure S5. Size distribution obtained by DLS analysis of a sample containing **3AL** (20 µM) and **1** (0.2 µM, 3.4-3.6 µM in the disaccharide repeating unit). The analyses of five replicates are shown.

ITC experiments with 3LL

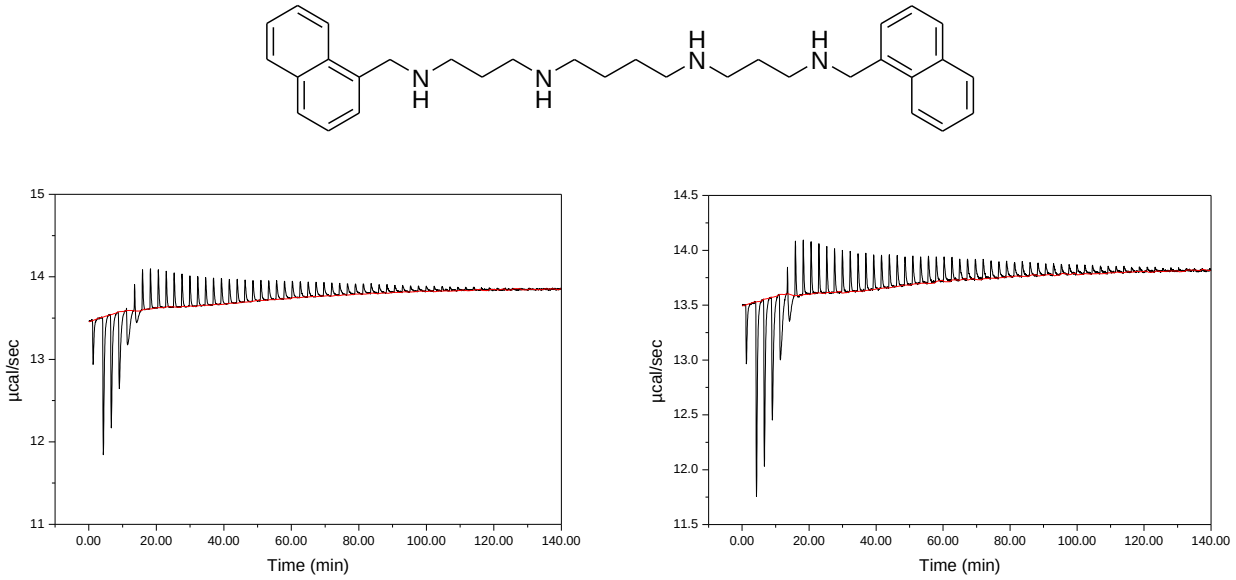

Figure S6. Raw data for two ITC experiments of **3LL** with heparin.

In this case, we were unable to fit the observed heat change to any available binding model. Moreover, the shape of the heat peaks during the experiment suggested a weaker and less specific interaction with heparin.

ITC experiments with 3AA

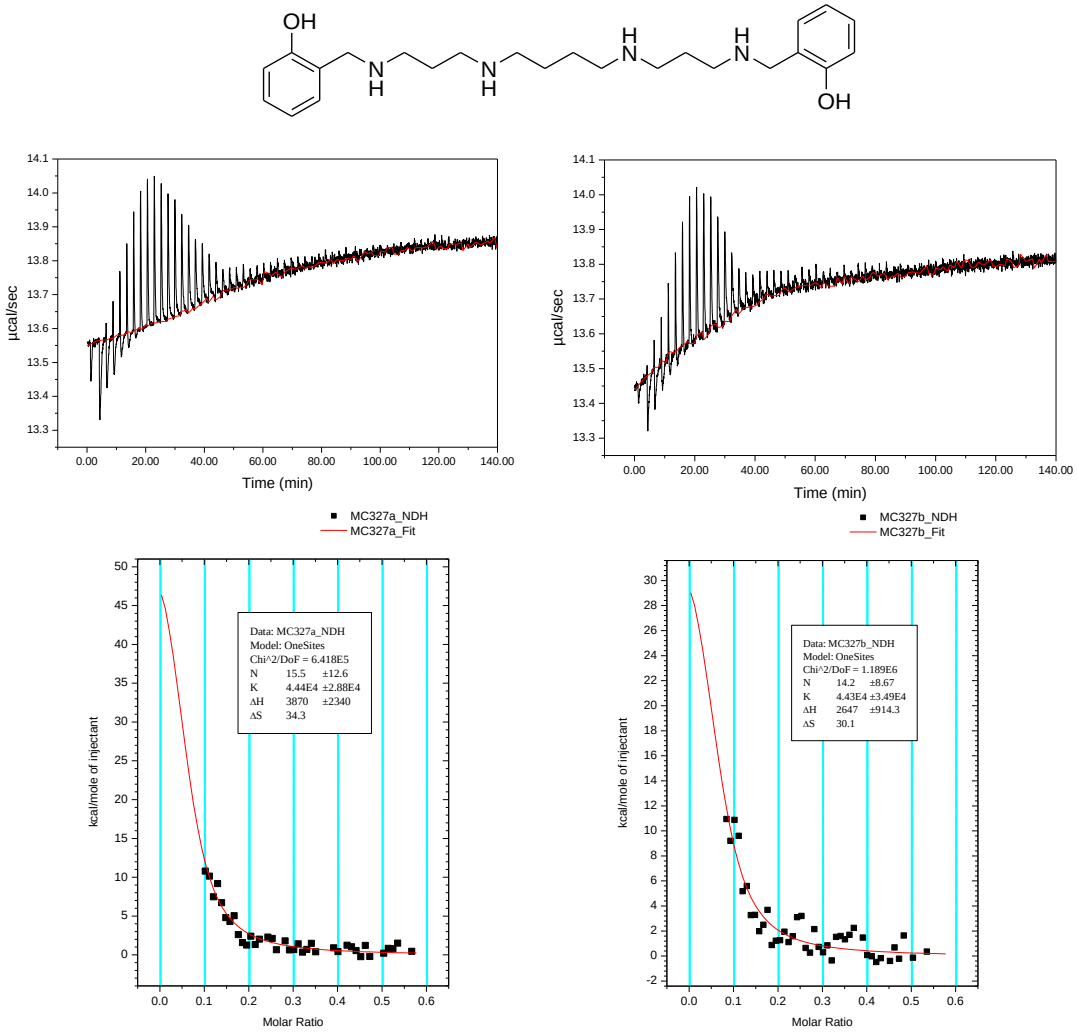

Figure S7. Raw data (up) and processed data (down) for two ITC experiments of **3AA** with heparin.

ITC results

Despite the fitting for **3AA** was not very accurate, we used the obtained values for comparison (Table S1). The results obtained from the fitting of the data for **3AL** and **3AA** clearly showed that **3AL** is a stronger binder to heparin, by at least one order of magnitude in the affinity (K_d) and a more favorable Gibbs energy (ca. 2 kcal/mol). Moreover, the apparently larger stoichiometry with **3AA** also reflects a less efficient interaction.

Table S1: Thermodynamic parameters obtained by fitting the ITC data to a simple one-site binding mode:

	3AL		**3AA**	
N	7.5±0.1	7.3±0.1	15.5±12	14.2±8
$K_{association}$ (M^{-1})	$8.34\cdot10^5\pm1.8\cdot10^5$	$6.89\cdot10^5\pm1.4\cdot10^5$	$4.44\cdot10^4\pm2.9\cdot10^4$	$4.43\cdot10^4\pm3.5\cdot10^4$
$K_{dissociation}$ (μM)	1.20±0.20	1.45±0.20	22.5±8.9	22.5±9.9
ΔH ($cal\cdot mol^{-1}$)	1858±42	1969±46	3870±2340	2647±914
ΔS ($cal\cdot K^{-1}\cdot mol^{-1}$)	33.3	33.3	34.3	30.1
ΔG ($cal\cdot mol^{-1}$)	-8065	-7954	-6351	-6333

NMR binding experiments

NMR characterization of 3AL in aqueous buffer

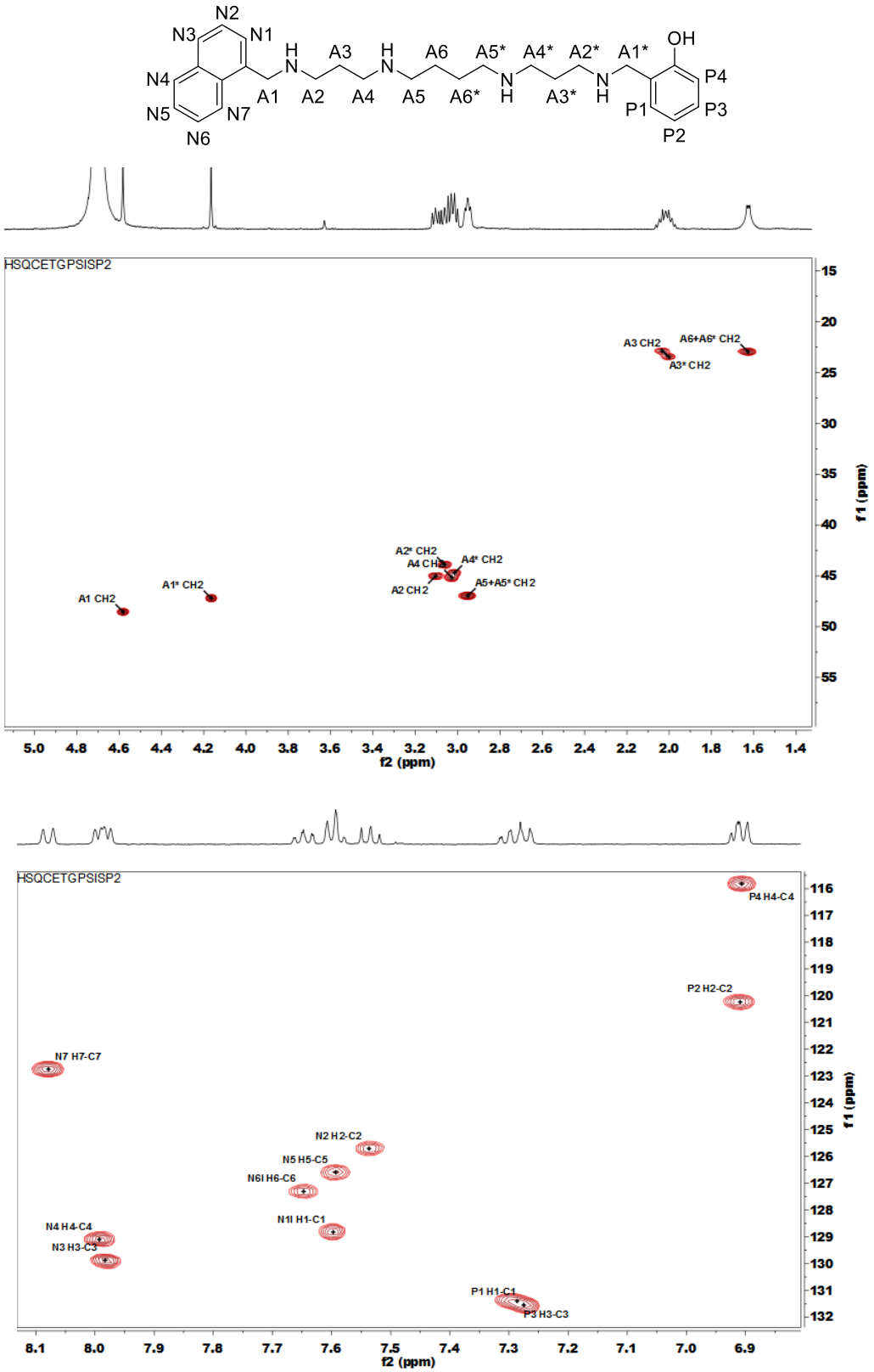

Figure S8. ^{1}H-^{13}C HMBC spectrum of compound **3AL** 1 mM (500 MHz, 5 mM Tris-d11 and 50 mM NaCl in D_20, pH 7.5) and chemical structure of **3AL** with labelling numbers used in the NMR assignment.

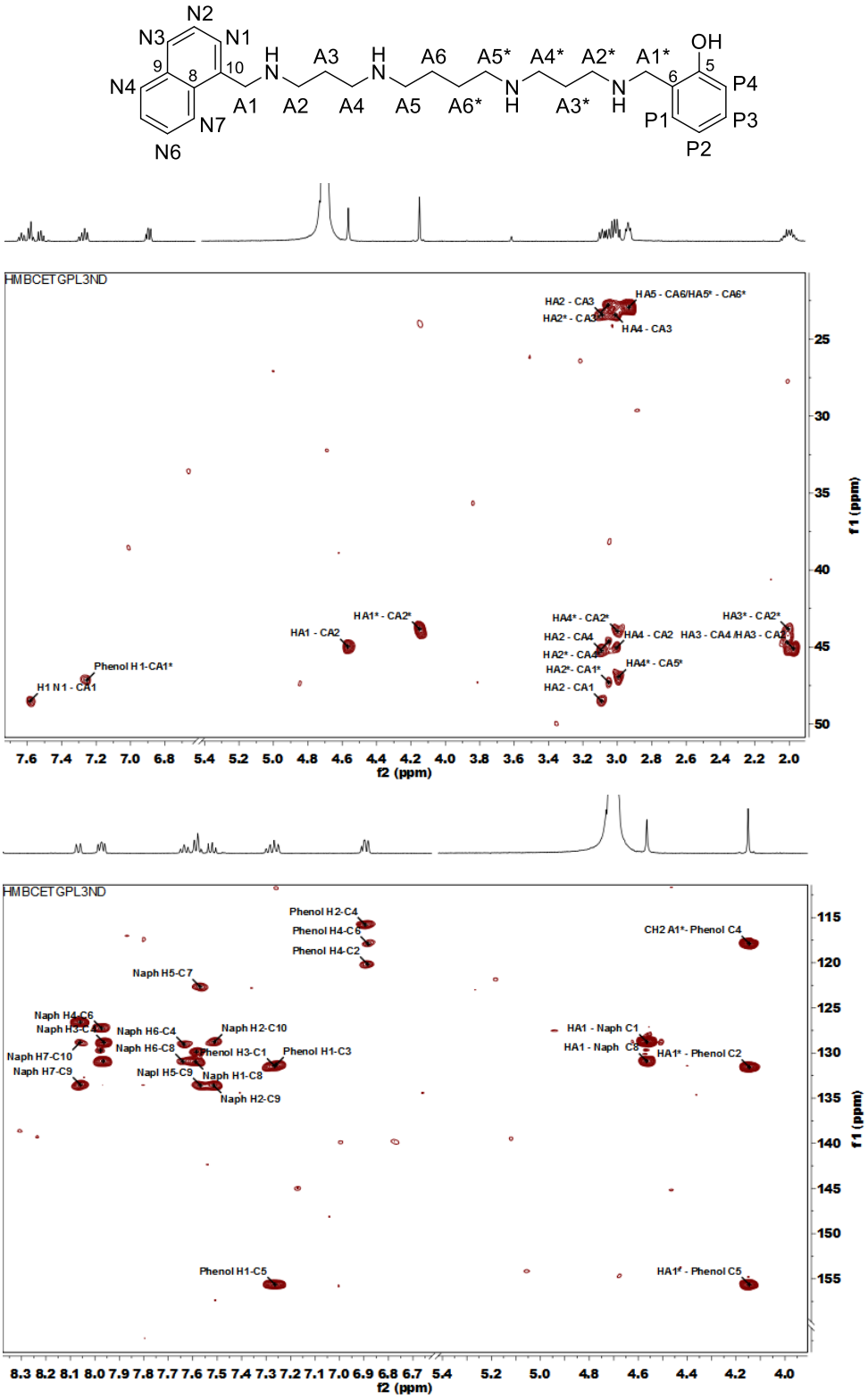

Figure S9. ^{1}H-^{13}C HSQC spectrum of compound **3AL** 1 mM (500 MHz, 5 mM Tris-d11 and 50 mM NaCl in D_20, pH 7.5) and chemical structure of **3AL** with labelling numbers used in the NMR assignment.

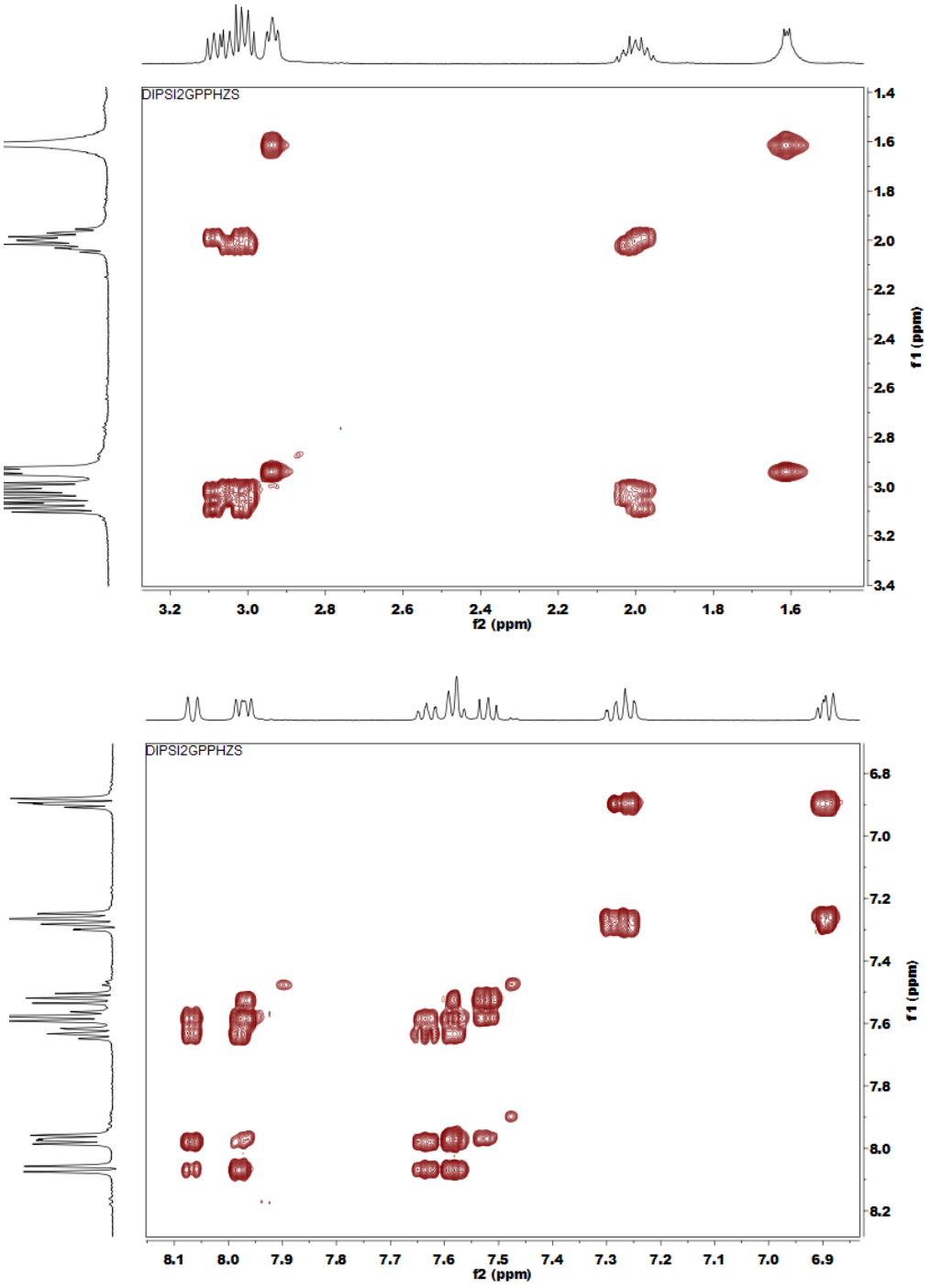

Figure S10. ^{1}H-^{1}H TOCSY spectrum of compound **3AL** 1 mM (500 MHz, 5 mM Tris-d11 and 50 mM NaCl in D_20, pH 7.5).

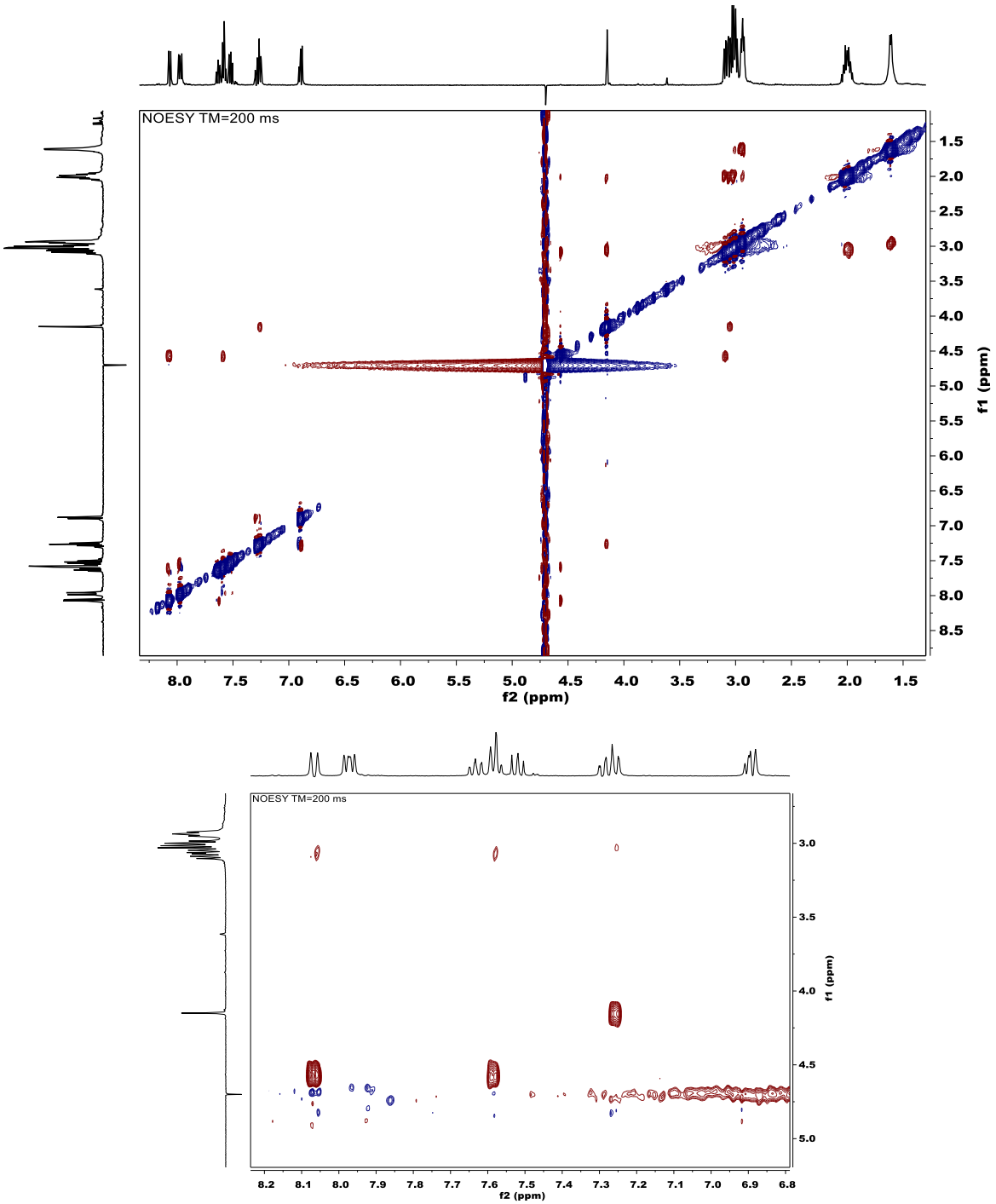

Figure S11. ^{1}H-^{1}H NOESY spectrum of compound **3AL** 1 mM (500 MHz, 5 mM Tris-d11 and 50 mM NaCl in D_20, pH 7.5).

3AL-heparin interaction studies by NMR

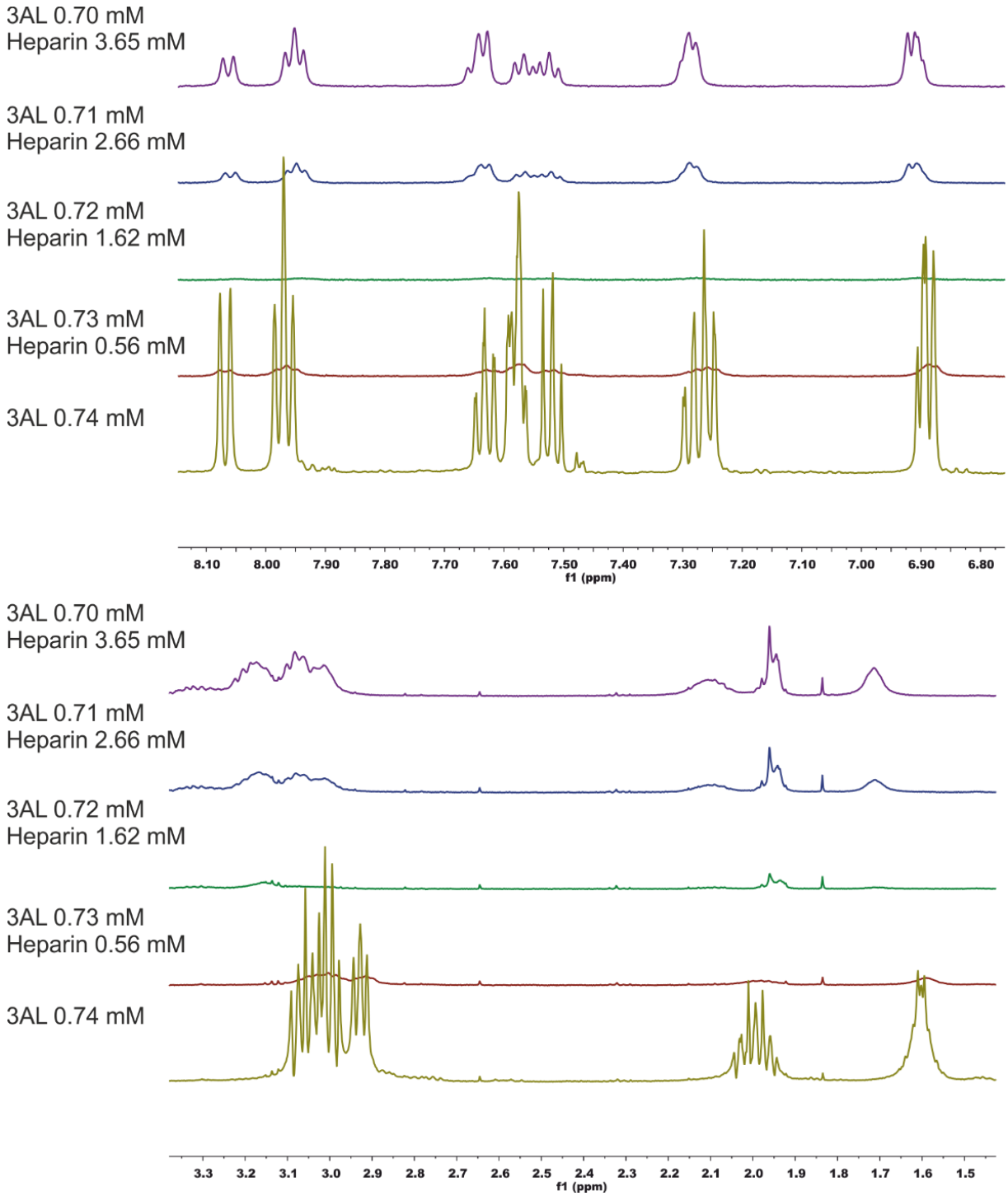

Figure S12. ^{1}H CPMGPR1D NMR spectra of compound **3AL** in the presence of increasing amounts of heparin. The concentrations of the heparin are referred to the concentration of the disaccharide repeating unit, considering the average molecular weight and the composition of the heparin sample here used. All spectra were acquired at 500 MHz in 5 mM Tris-d11 and 50 mM NaCl in D_20, pH 7.5.

3AL-dp14 heparin interaction studies by NMR

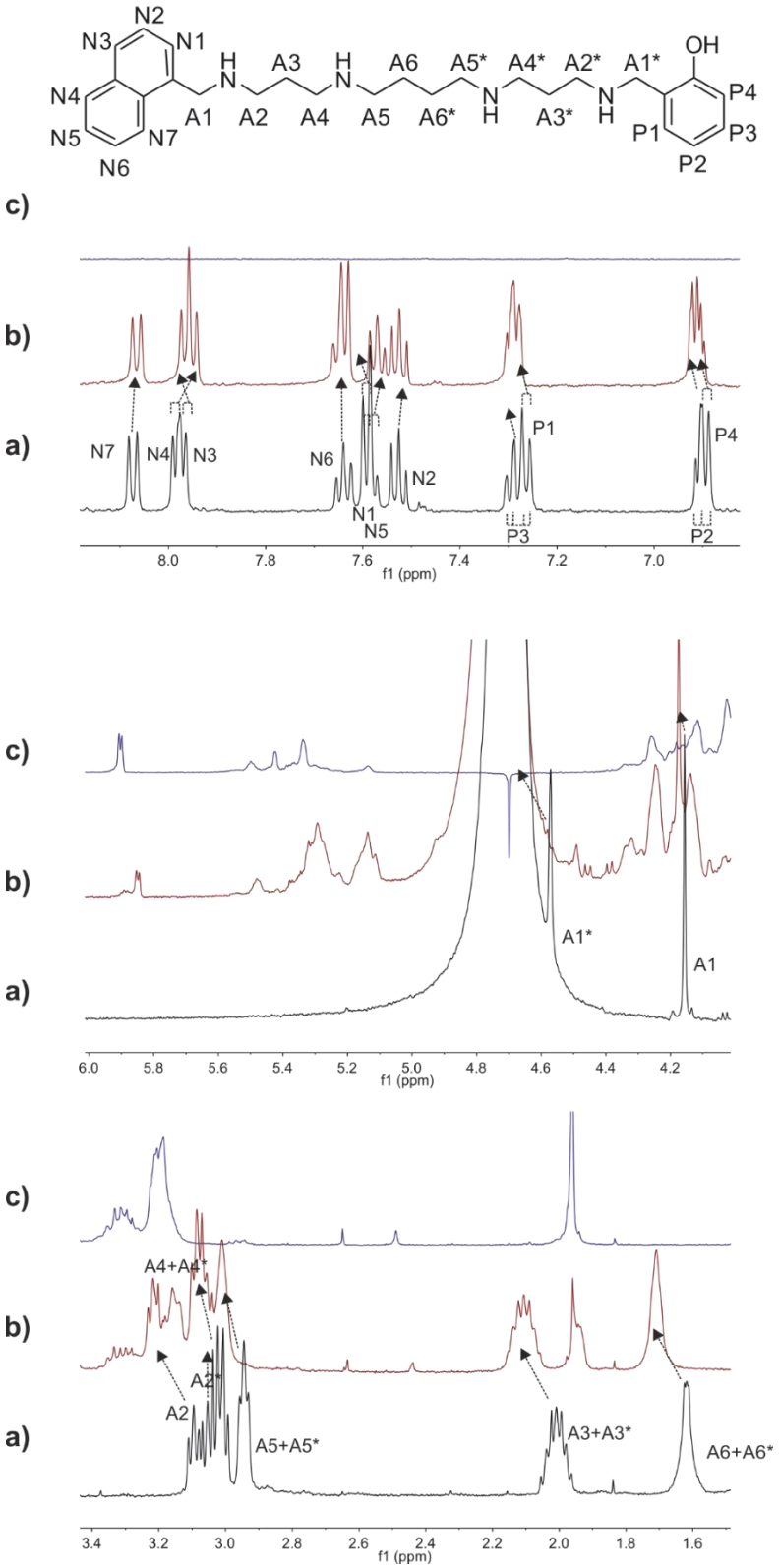

Figure S13. Selected regions of the ^{1}H NMR spectra of: (a) compound **3AL** (0.55 mM) (c) **dp14** heparin (2.8 mM in the corresponding disaccharide repeating unit) and (b) mixture of **3AL** and **dp14**. All spectra were acquired at 500 MHz in 5 mM Tris-d11 and 50 mM NaCl in D_20, pH 7.5.

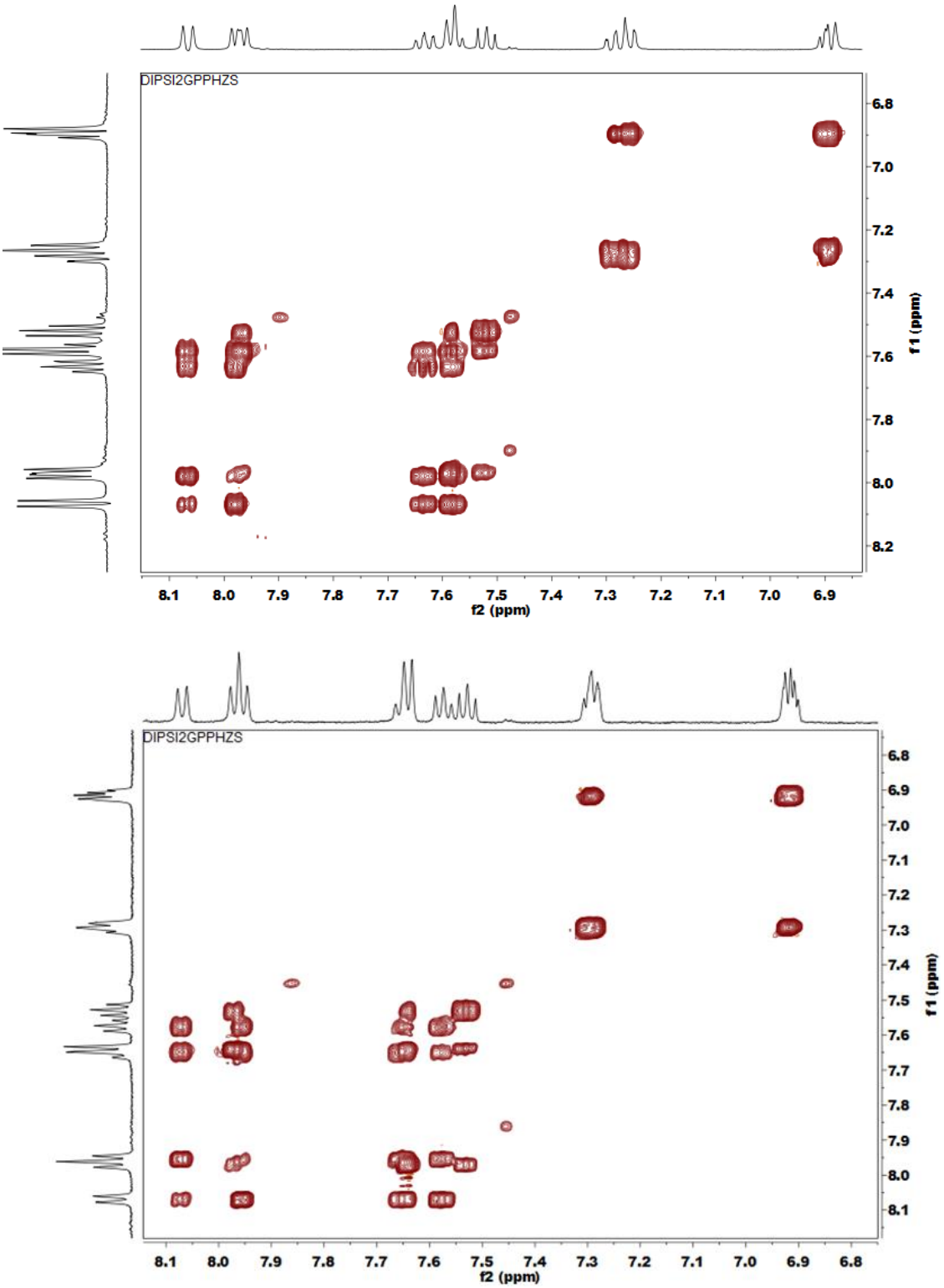

Figure S14. ^{1}H-^{1}H TOCSY spectrum (500 MHz, 5 mM Tris-d11 and 50 mM NaCl in D_20, pH 7.5) of compound **3AL** (0.55 mM) in the presence of **dp14** heparin (2.8 mM in the corresponding disaccharide repeating unit).

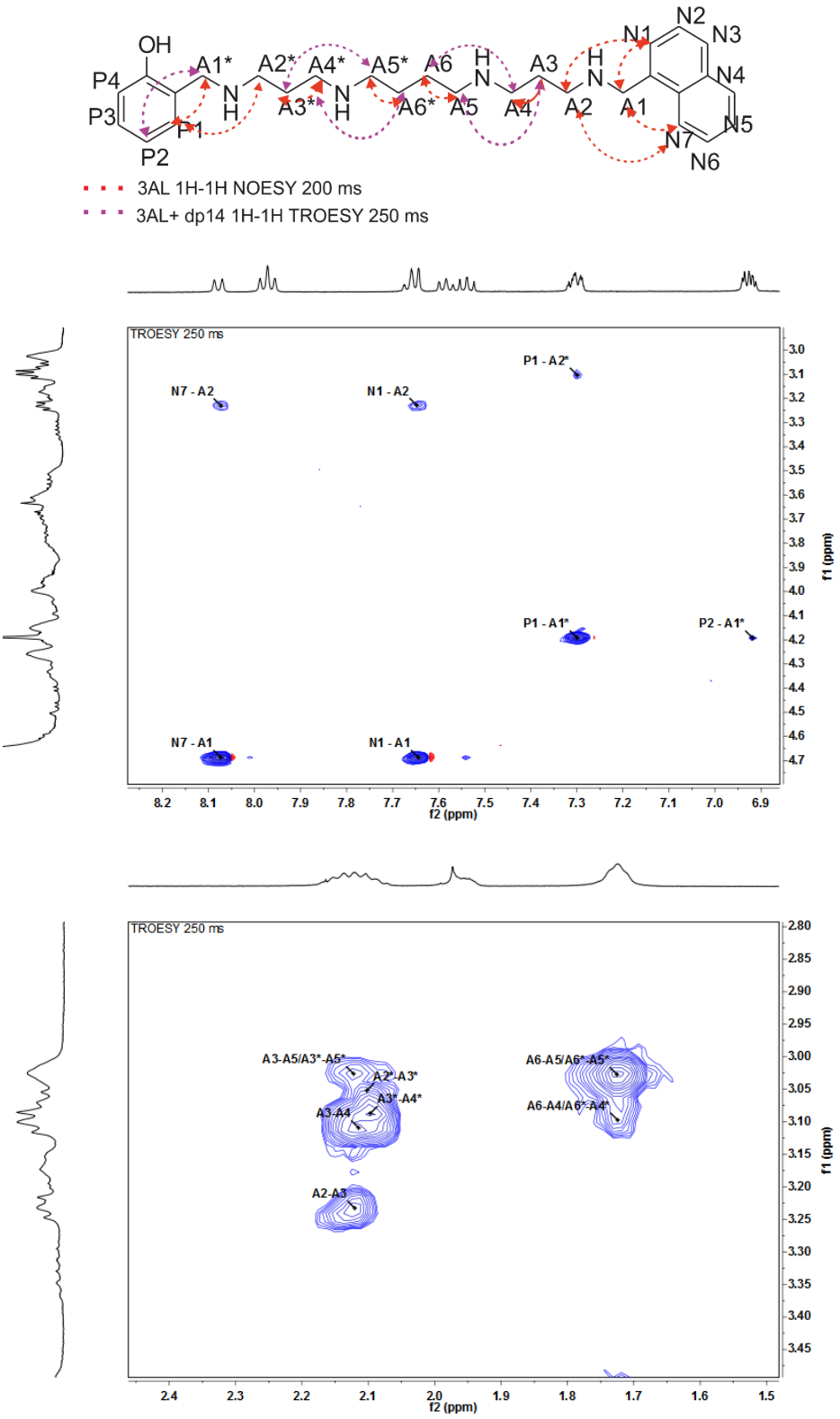

Figure S15. ^{1}H-^{1}H TROESY spectrum (500 MHz, 5 mM Tris-d11 and 50 mM NaCl in D_20, pH 7.5) of compound **3AL** (0.55 mM) in the presence of **dp14** heparin (2.8 mM in the corresponding disaccharide repeating unit).

Blood coagulation factor enzymatic assays

Recombinant antithrombin III and coagulation Factor Xa were obtained from the Berichrom Heparin test, supplied by SIEMENS. Following the indications of the test kit, stock solutions were prepared as follows: Human antithrombin III (1 IU/mL), Factor Xa reagent (0.4 µg/mL, human plasma fraction with the additives Tris, sodium chloride and EDTA) and a chromogenic substrate specific for factor Xa (4 mM of Z-D-Leu-Gly-Arg-ANBA-methyl amide). On the other hand, 4-nitroaniline (Sigma Aldrich) was added to the substrate solution at a concentration of 1.6 mM and was used as internal standard to quantify the cleavage of the chromogenic substrate. Heparin (sodium salt from porcine intestinal mucosa, polydisperse, from 6000 to 30000 Daltons) was purchased from Sigma-Aldrich. All compounds were dissolved in miliQ water at the desired stock concentrations prior to start the assays and kept at 4℃.

Various concentrations of the ligand (**3AL** or **3AA**), heparin (0.4 IU/mL or 0.6 IU/mL), human antithrombin III solution (10 µL) and Factor Xa reagent solution (100 µL) were added in that order in an Eppendorf and brought to a total volume of 120µL. Then, 40 µL of Reagent Substrate solution was added to start the experiment and the mixture was vigorously shaken at 25℃. 20 µL samples were taken at minutes 5/10/15/20/30/50/80/120, diluted with 40 µL of acetic acid (20% v/v), and injected in the analytical HPLC. The gradient ranged from 5% of ACN (0.1% formic acid) in water (0.1% formic acid) to 100% of ACN in 24 minutes using a 15 x 4.6 mm KROMAPHASE C18 5.0 µm column (retention time of cleaved chromophore 9.1 min, retention time of chromogenic substrate 13.9min, retention time of 4-nitroaniline 15.4min).

FXa/ATIII activity was represented as percent of hydrolysis, which was calculated from the normalized area of cleaved peptide at 405 nm at each corresponding time point. Experiment carried out in absence of heparin was considered as maximum of activity while experiment with heparin and no ligand was considered as negative control (maximum inhibition of FXa by heparin). Concentration of heparin was selected for the measurement to render a significant inhibition within experimental time, while allowing the reaction to proceed.

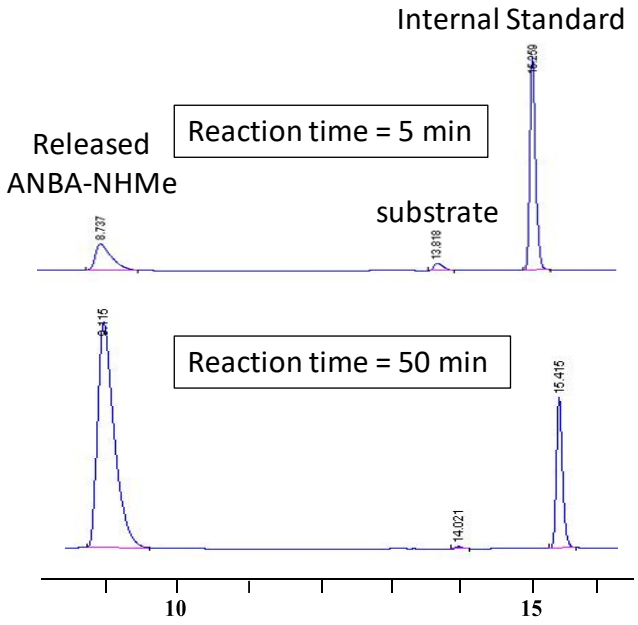

Figure S16. Typical HPLC traces showing the progression of the hydrolysis reaction

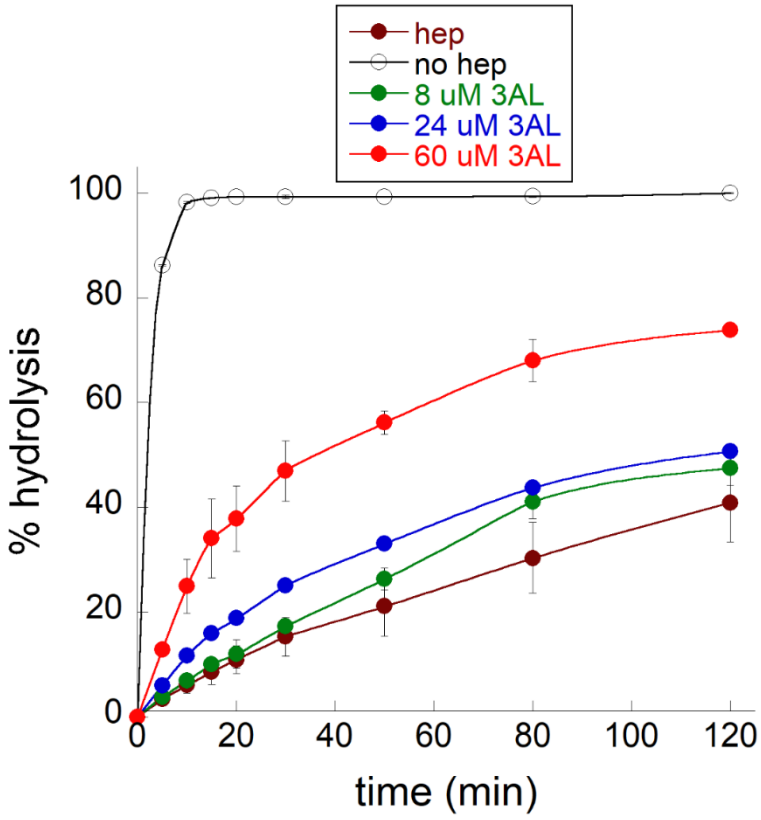

Figure S17. Plot of the percent of the hydrolysis of the Z-D-Leu-Gly-Arg-NMe-AMBA peptide (measured by HPLC at 405 nm) catalyzed by the FXa/AT_{III} system in the absence (black) or in the presence of 0.6 IU/mL **1** (brown). Increasing concentrations of the ligand **3AL** (green 8 μM, blue 24 μM, red 60 μM) produces an increase of the rate of the hydrolysis of the peptide, which is lower than in the presence of a smaller amount of heparin (compare with Figure 4B of the manuscript).

Another control experiment was performed with **3AL**. A reaction was carried out with 0.4 IU/mL of heparin and 8 μM **3AL**, also containing AT_{III}, FXa and the peptide substrate Z-D-LGR-N(Me)ANBS. The additional background reactions without heparin (maximum activity of FXa enzyme) or with heparin but without **3AL** (maximum inhibition of FXa by heparin) were also done within the same batch. The percent of hydrolysis was monitored at different time points as in the previous cases. After 120 minutes, a 50% additional heparin was added to the two reactions that initially contained heparin (with/without **3AL**), whereas new fresh substrate was added to the three reaction vessels, and the evolution of the hydrolysis was monitored for other 120 minutes. The normalized hydrolysis of the peptide substrate (corrected considering the amount of hydrolyzed substrate already present in the reaction) showed that the presence of additional heparin induced a much efficient inhibition of the FXa enzyme. These results unambiguously show that the ligand **3AL** only binds heparin and has no other unexpected effects on the enzymatic assay.

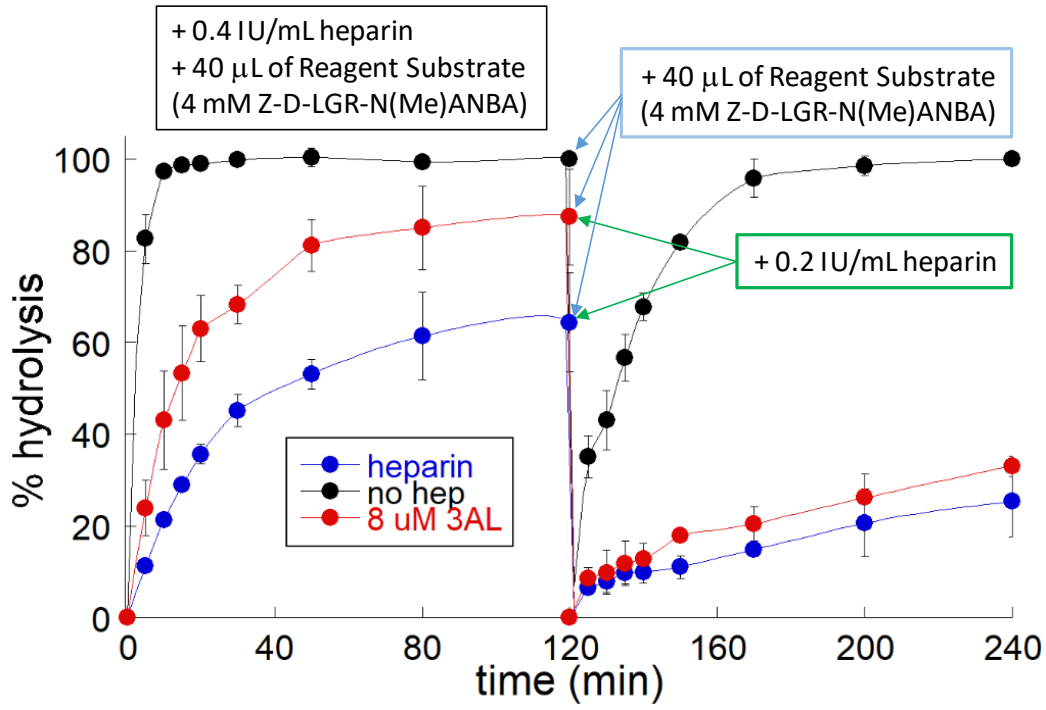

Figure S18. Plot of the percent of the hydrolysis of the Z-D-Leu-Gly-Arg-NMe-AMBA peptide (measured by HPLC at 405 nm) catalyzed by the FXa/AT_{III} system in the absence (black) or in the presence of 0.4 IU/mL of **1** (blue). Addition of the ligand **3AL** (red 8 μM) induced the partial recovery of the enzymatic activity. At 120 min, additional heparin (+0.2 IU/mL) was added to the two reactions that already contained heparin, whereas peptide substrate was added to all the reactions. The percent of the hydrolysis of the substrate (normalized and corrected) showed a decrease of the enzymatic activity.

Molecular Dynamics Simulation Methods

All molecular simulations were carried out with the package Schrödinger Suite 2017,[3] through its graphical interface Maestro.[4] The program Macromodel,[5] with its default force field OPLS3[6] and GB/SA water solvation conditions,[7] was used for energy minimization. Molecular dynamics simulations were performed with the program Desmond,[8] using the OPLS3 force field. A heparin hexadecamer model (**dp16**) was derived from residues 3-19 of chain A of the reported solution structure of heparin DP36 (PDB 3IRL).[9] Ligand **3AL** was built within Maestro. Heparin **dp16** was modelled with all its sulfate and carboxylate groups in their ionized state (-32 total charge), while the **3AL** ligand was modelled with its four amino groups protonated, as suggested by pKa calculations carried out with Epik.[10] Both structures were energy minimized before building the simulation system. To approach the high stoichiometric ratio of the heparin-3AL complex determined in our ITC experiments, a system composed of a **dp16** molecule plus five unbound and arbitrarily placed **3AL** molecules was set up in a cubic box whose sides were at 15 Å of the closest solute atom, with added Na^+ ions to reach neutrality and the whole system solvated with TIP3P water (~26300 TIP3P molecules), using the System Builder of the Maestro-Desmond interface.[11]

The full system (~80000 atoms) was subjected to steepest descent minimization, first with the solute restrained and then without restraints until a gradient threshold of 0.1 kcal/mol/Å was reached. Then it was heated stepwise until 300 K with short MD runs under periodic boundary conditions (PBC, NPT, Berendsen thermostat-barostat) (12 ps at 0.1, 10, 100 and 300 K), and equilibrated for 2 ns at the last temperature and 1.0 bar in the NPT ensemble. A production MD simulation (500 ns, 2 fs time step) was performed under the same conditions (PBC, NPT ensemble, 300 K and 1.0 bar) using the Nose-Hoover thermostat method[12] with a relaxation time of 1.0 ps and the Martyna-Tobias-Klein barostat method[13] with isotropic coupling and a relaxation time of 2 ps. Integration was carried out with the RESPA integrator[14] using time steps of 2.0, 2.0, and 6.0 fs for the bonded van der Waals and short range and long range electrostatic interactions, respectively. A cut-off of 9 Å was applied to van der Waals and short-range electrostatic interactions, while long-range electrostatic interactions were computed using the smooth particle mesh Ewald method with an Ewald tolerance of 10^{-9}.[15] Bond lengths to hydrogen atoms were constrained using the Shake algorithm.[16] Coordinates were saved every 200 ps, hence 2500 snapshots (frames) were obtained. The Simulation Event Analysis application included in the Desmond-Maestro interface and different ad-hoc scripts were used to analyze the simulations results. The 2500 snapshots were clustered based on the atomic RMSD of the heavy atoms using the hierarchical clustering with average linkage method implemented in the Schrodinger Suite and fixing the number of clusters to 10.

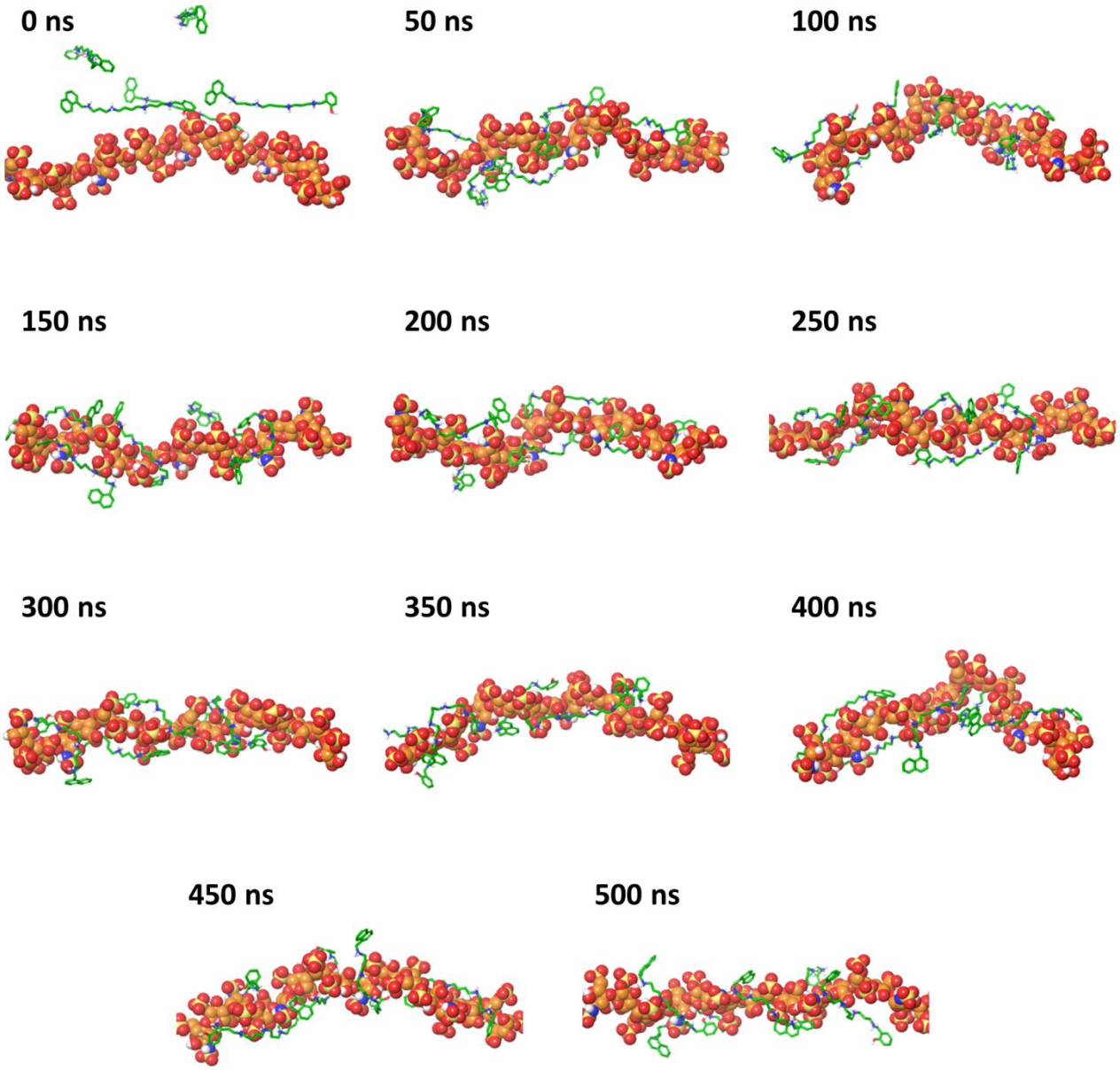

Figure S19. Snapshots from the 500 ns MD simulation of a system containing one **dp16** heparin model (spheres) and five 3AL (green sticks) molecules. Water molecules and ions are omitted for clarity.

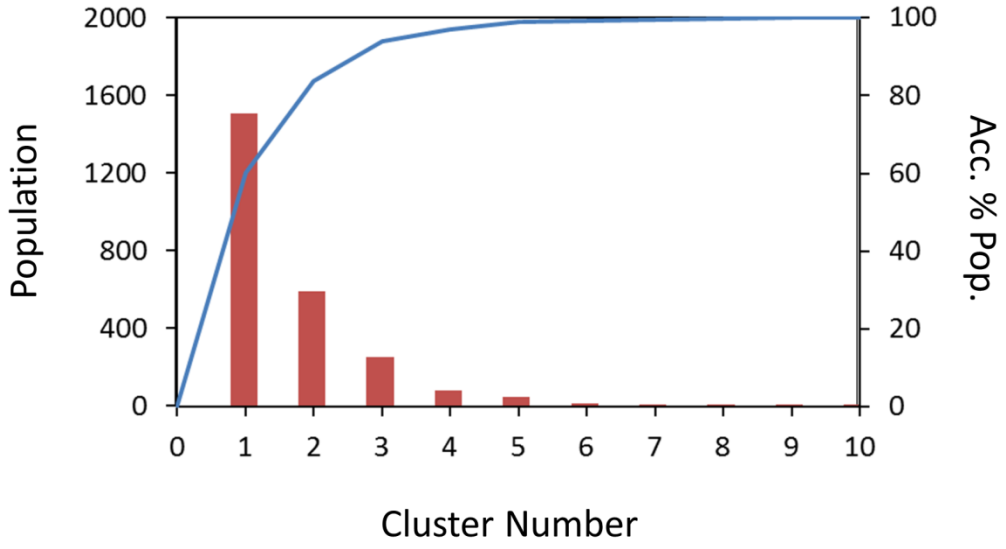

Figure S20. Results from clustering the 2500 snapshots obtained from molecular dynamics, by applying a hierarchical clustering method with 10 clusters. The graph shows the population distribution among the clusters (red bars, left axis) and the accumulated % of population (blue line, right axis).

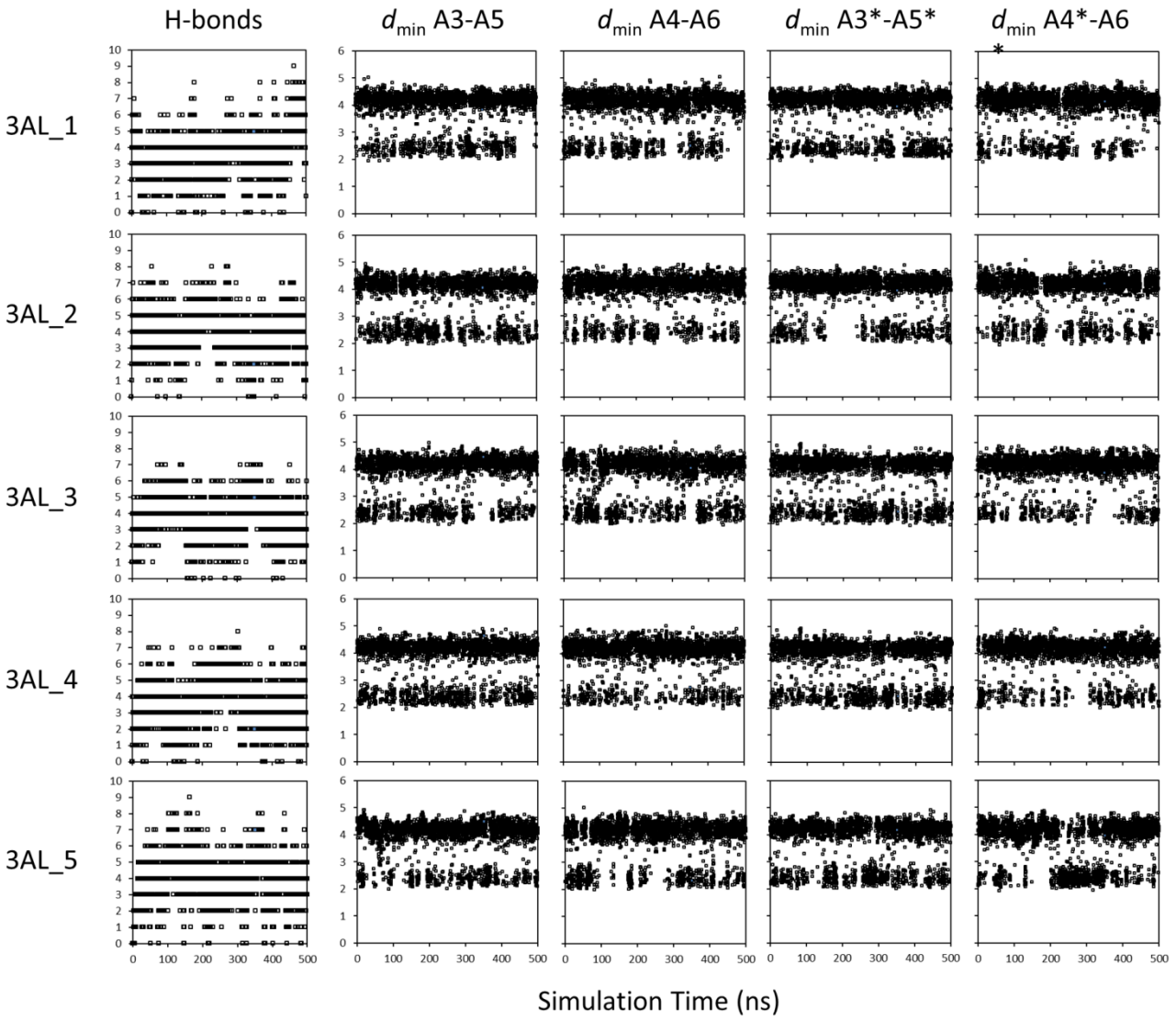

Figure S21. Results from molecular dynamics. For each of the five **3AL** molecules in the simulation, the graphics show the dependence on simulation time of: (1) the number of hydrogens bonds established with **dp16** (averages for the whole simulation: 3.5±1.5 (3AL_1), 4.0±1.4 (3AL_2), 3.8±1.4 (3AL_3), 3.6±1.6 (3AL_4) and 3.8±1.6 (3AL_5)) and (2) the minimum distance (Å) between protons on positions A3 and A5, A4 and A6, A3* and A5*, and A4* and A6*.

References.

[1] G. Klocek, J. Seelig, *Biochemistry* **2008**, *47*, 2841-2849.

[2] M. Corredor, R. Bonet, A. Moure, C. Domingo, J. Bujons, I. Alfonso, Y. Pérez, À. Messeguer, *Biophysical Journal* **2016**, *110*, 1291-1303.

[3] Schrödinger, Schrödinger, LLC, New York, NY, **2017**.

[4] Schrödinger, Schrödinger, LLC, New York, NY, **2017**.

[5] Schrödinger, Schrödinger, LLC, New York, NY, **2017**.

[6] E. Harder, W. Damm, J. Maple, C. Wu, M. Reboul, J. Y. Xiang, L. Wang, D. Lupyan, M. K. Dahlgren, J. L. Knight, J. W. Kaus, D. S. Cerutti, G. Krilov, W. L. Jorgensen, R. Abel, R. A. Friesner, *Journal of chemical theory and computation* **2016**, *12*, 281-296.

[7] W. C. Still, A. Tempczyk, R. C. Hawley, T. Hendrickson, *J. Am. Chem. Soc.* **1990**, *112*, 6127-6129.

[8] aSchrödinger, D. E. Shaw Research, New York, NY, **2017**; bK. J. Bowers, E. Chow, H. Xu, R. O. Dror, M. P. Eastwood, B. A. Gregersen, J. L. Klepeis, I. Kolossváry, M. A. Moraes, F. D. Sacerdoti, J. K. Salmon, Y. Shan, D. E. Shaw, in *Proceedings of the ACM/IEEE Conference on Supercomputing (SC06)*, Tampa, Florida, **2006**.

[9] S. Khan, J. Gor, B. Mulloy, S. J. Perkins, *J Mol Biol* **2010**, *395*, 504-521.

[10] aSchrödinger, Schrödinger, LLC, New York, NY, **2017**; bJ. R. Greenwood, D. Calkins, A. P. Sullivan, J. C. Shelley, *J. Comput. Aided Mol. Des.* **2010**, *24*, 591-604; cJ. C. Shelley, A. Cholleti, L. L. Frye, J. R. Greenwood, T. M. R., M. Uchiyama, *J. Comput. Aided Mol. Des.* **2007**, *21*, 681-691.

[11] Schrödinger, D. E. Shaw Research, New York, NY, **2017**.

[12] aD. J. Evans, B. L. Holian, *The Journal of Chemical Physics* **1985**, *83*, 4069-4074; bG. J. Martyna, M. L. Klein, M. Tuckerman, *The Journal of Chemical Physics* **1992**, *97*, 2635-2643.

[13] G. J. Martyna, D. J. Tobias, M. L. Klein, *The Journal of Chemical Physics* **1994**, *101*, 4177-4189.

[14] M. Tuckerman, B. J. Berne, G. J. Martyna, *The Journal of Chemical Physics* **1992**, *97*, 1990-2001.

[15] aT. Darden, D. York, L. Pedersen, *The Journal of Chemical Physics* **1993**, *98*, 10089-10092; bU. Essmann, L. Perera, M. L. Berkowitz, T. Darden, H. Lee, L. G. Pedersen, *The Journal of Chemical Physics* **1995**, *103*, 8577-8593.

[16] V. Kräutler, W. F. van Gunsteren, P. H. Hünenberger, *Journal of Computational Chemistry* **2001**, *22*, 501-508.